Received: 6 September 2019 | Revised: 18 November 2019 | Accepted: 26 November 2019

DOI: 10.1002/aoc.5444

Applied Organometallic Chemistry WILEY

FULL PAPER

Synthesis, DFT, computational exploration of chemical reactivity, molecular docking studies of novel formazan metal complexes and their biological applications

Shakeel Ahmad Khan[1,2] | **Komal Rizwan**[3] | **Sammia Shahid**[1] | **Mahmoud A. Noamaan**[4] | **Tahir Rasheed**[5] | **Hira Amjad**[1]

[1]Department of Chemistry, School of Science, University of Management and Technology, Lahore, 54770, Pakistan

[2]Center of Super Diamond and Advanced Films (COSDAF), Department of Chemistry, City University of Hong Kong, 83 Tat Chee Avenue, Kowloon, China

[3]Department of Chemistry, Government College Women University, Faisalabad, 38000, Pakistan

[4]Mathematics Department, Faculty of Science, Cairo University, Giza, 12613, Egypt

[5]School of Chemistry and Chemical Engineering, State Key Laboratory of Metal Matrix Composites, Shanghai Jiao Tong University, Shanghai, 200240, China

Correspondence
Shakeel Ahmad Khan, Department of Chemistry, School of Science, University of Management and Technology, Lahore-54770, Pakistan.
Email: shakilahmadkhan56@gmail.com
Komal Rizwan, Department of Chemistry, Government College Women University, Faisalabad, 38000, Pakistan.
Email: komal.rizwan45@yahoo.com

The computational exploration of chemical reactivity and molecular docking of the synthesized formazan compounds **(S1-S6)** were studied. Further, their antimicrobial activity against bacterial strains (*S. epidermidis*, *B. cereus*, *K. pneumoniae* and *P. aeruginosa*) and against fungal strains (*T. mentagrophytes*, *C. albicans*, *A. niger*, *S.* cerevisiae and *C. glabrata*) using agar diffusion method and antioxidant activity following DPPH inhibition assays were evaluated. Anticancer activity was executed in *vitro* model of human breast carcinoma (MCF-7) cell line. The superior and enhanced antibacterial and antimycotic activities were exhibited by formazan compound **(S4)** by presenting maximum ZOIs and MICs values. While enhanced antioxidant in terms of percentage inhibition of DPPH and cytotoxic effect on human breast carcinoma-cells demonstrated by formazan compound **(S1)** which was further validated by the results of molecular docking studies of **(S1)** with the human estrogen receptor protein. In order to compute quantum chemical reactivity descriptors from conceptual density functional theory (CDFT) point of view of this system, including chemical potential (μ), chemical hardness (η), electrophilicity (ω), condensed Fukui function and dual descriptors are calculated at the same level of calculation. The most active sites of these molecules are determined and correlated with experimental data. The present investigation displays that formazans compounds could be potential drug candidate that constrains the growth of microbial strains, possess ability to cause cytotoxic effect on carcinoma cells and act as effective scavenger for free radical species.

KEYWORDS

anticancer, antimicrobial, DFT studies, formazan, molecular docking

1 | INTRODUCTION

Now days, development of multi-drug resistance in several bacterial strains including *salmonella, streptococci, gonococci, enterococci, staphylococci* etc. has become an emerging issue. Besides, some fungi for example *Candida* species are also displaying resistance to various antifungal drugs.[1] Numerous antimicrobial drugs have been developed however; because of the emergence of multidrug-resistance in pathogens, clinical-efficiency of

the existing drugs is being vulnerable.[2] According to World Health Organization (WHO), if we could not develop efficient drugs to control or destroy microbes, the death caused by microbial diseases may rise to millions by 2020. Regarding this, it has become obligatory to find out alternate routes to tackle these multi-drug resistant microbes.[1] In addition to deaths due to microbial diseases, cancer is also one of the prime factor for the deaths in human beings. Literature survey reveals that international cancer burden has become twice during the period of 1975 to 2000, and will double again by 2020.[3] Even though, significant advancements have been taken place in cellular and molecular biology which have improved the chemotherapeutic treatments of cancer but persistent determination is still obligatory to discover new-fangled anticancer drugs.[4–7]

The azomethine and its derivatives have been considered as a protuberant research objects due to their significant complexometric behavior and pharmacological physiognomies.[8] Azomethine derivatives perform noteworthy role by demonstrating numerous biological activities such as anticonvulsant, antiviral, antimicrobial, antioxidant, antitubercular, anticancer, anti-HIV, anthelmintic and anti-inflammatory. Azomethines are to be considered as an important intermediate for the development of different kinds of biological active derivatives viz. formazans, pyrazolines, thiazolidinones, azetidinones and isoxazolines.[8–12] Formazans and their derivatized molecular structures are highlighted a lot because of their noteworthy pharmaceutical and therapeutic potentials as an antifertility,[13] antioxidants,[14] antibacterial,[9,10] antifungal,[10] antiviral,[15] antiparkinsonian,[16] antitubercular,[17] anticonvulsant,[18] anti HIV,[19] anticancer,[20] antihyperglycemic,[21] antiproliferative,[22] analgesic and anti-inflammatory agents.[23–27] Several reports are available on formazans and their derivatives for biological applications, however very few reports are on formazan metal complexes.[28]

Formazans are typically synthesized in two steps; diazotization of aromatic amines followed by coupling with the hydrazones (coupler agent).[29,30] Hydrazones are synthesized by the condensation reaction of hydrazines and aldehydes in the presence of catalysts i.e. NaOH, Na_2CO_3, Betaine HCl, TsOH etc. under high temperature conditions with prolonged reaction time (1 hr to 3 hr approximately). The limitations of this approach are high temperature, long reaction time, modest yield, environmental incompatibility, and the usage of toxic chemical entities. Now days, much attention has been considered for exploiting biocompatible or bionature materials as catalyst or solvent in organic reactions.[31] In this regards, Gu et al. has introduced the solution of meglumine and gluconic acid as promoting medium for the reaction of formaldehyde and β-ketosulfones.[32] Meglumine is a promising contender as it have eco-friendly properties such as physiological inertness and biodegradability. Moreover, meglumine is amino sugar derivative of sorbitol, which could be employed as an excipient in different pharmaceutical formulations and with the combination of iodinated compounds because of its low toxicity. Meglumine is economical, non-toxic, stable to moisture and air, and can be easily availed from commercial market.[33] Recently, meglumine has widely explored as an efficient catalyst for the synthesis of several organic compounds such as pyrazoles, dihydro-pyridines, pyrazolo-pyranopyrimidines, pyranopyrazole derivatives and 2-amino-4H-pyrans.[34–38]

We aimed to synthesize metal complex formazans by following simple, efficient and environment friendly approach. For this, first we have synthesized the aromatic hydrazone (coupling agent) employing meglumine (biocompatible) as a catalyst, which further reacted with aromatic diazonium salt to produce formazans. Upon metallization reaction with different metal salts, metal complex formazans were synthesized which were then evaluated for their biomedical applications such as antibacterial, antifungal, and anticancer. The structural properties of formazans were also studied through DFT calculations and molecular docking studies.[39]

2 | EXPERIMENTAL

2.1 | Chemicals

The chemicals and reagents exploited in this work have been purchased from Sigma Aldrich and.

Fluka Chemische (Switzerland). They are all of analytical grade.

2.2 | Generalized protocol for the synthesis of hydrazone 4-[(2Z)-2-benzylidenehydrazinyl] benzene sulfonic acid (BASAH)

The hydrazone **(BASAH)** was prepared by the reduction of diazonium salt **(SAD)** of 0.1 mole of 4-aminobenzenesulphonic acid **(SA)** into 4-hydrazinylbenzenesulfonic acid **(SAH)** which upon condensation with benzaldehyde **(BA)** in the presence of meglumine (0.15 mole), and C_2H_5OH/H_2O (1:1, 400 ml) at room temperature yielded resultant product **(BASAH)** as presented in Scheme 1.

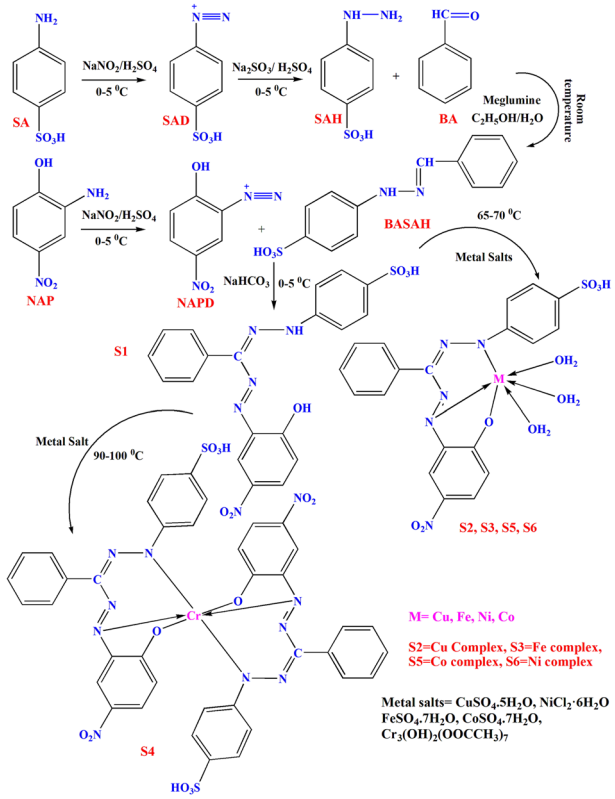

SCHEME 1 Synthesis of formazan and metallized formazan complexes **(S1-S6)**

2.2.1 | Synthesis of diazonium salt (SAD) and 4-hydrazinylbenzenesulfonic acid (SAH)

The diazonium salt **(SAD)** and 4-hydrazinylbenzenesulfonic acid **(SAH)** was synthesized following the procedure as described by[9,10] with slight modifications. For the synthesis of diazonium salt **(SAD),** the aqueous solution of 0.1 mole of **(SA)** was diazotized in the presence of $NaNO_2$ (7.3 g) and H_2SO_4 (20 ml) at 0–5 °C. Further, the hydrazine compound **(SAH)** was obtained by the reduction of already synthesized moist diazonium salt **(SAD)** in the presence of Na_2SO_3 (56.5 g) and H_2SO_4 (33.2 ml) at 0–5 °C (Scheme 1). Purification of the hydrazine compound **(SAH)** was accomplished following the protocol.[29,30]

Compound **(SAH)**; Off white powder. Yield = 95%. Melting point = 286 °C. FTIR (KBr, Cm^{-1}); 1385 (SO_3H), 3486 (N-H), 1604 (aromatic C=C), 3012 (aromatic C-H). ^{1}H-NMR (D_2O, 400 MHz) δ: 6.96 to 7.68 = Ar-H (m 4H), 11.19 = SO_3H (s 1H), 4.20 = N-H (s 1H), 1.40 = N-H (s 2H). ^{13}C-NMR (D_2O, 75 MHz) δ: 114.5, 114.5, 128.6, 128.6, 140.2, 154.8 (Aromatic carbons). Anal. Calc. for $C_6H_8N_2O_3S$ (Molecular weight = 188.2 $gmol^{-1}$): S = 17.04, *N* = 14.88, O = 25.50, H = 4.28, C = 38.29% and Found: S = 17.01, *N* = 14.81, O = 25.41, H = 4.25, C = 38.23%.

2.2.2 | Synthesis of hydrazone compound (BASAH)

The hydrazone **(BASAH)** was synthesized by the condensation reaction of compound **(SAH)** and benzaldehyde (Scheme 1).[33] In typical procedure, 0.1 mole of compound **(SAH)** (93% purity) dissolved in C_2H_5OH/H_2O (1:1, 400 ml). Subsequently, 0.15 mole of meglumine was added in the reaction mixture. Afterwards, 0.1 mole of benzaldehyde was added dropwise in the reaction mixture in 10 min. The reaction mixture was stirred at room temperature for reaction completion. The reaction was monitored continuously through thin layer chromatography (TLC). The reaction was completed within 30 min. After reaction completion, C_2H_5OH/H_2O (1:1, 50 ml) was added and the final product was extracted using C_2H_5COOH (30 ml). The anhydrous Na_2SO_4 was used for the amputation of organic phase and solvent was removed under vacuum conditions. The final product was purified by recrystallization process described by.[29,30]

Pale yellow powder. Yield = 96%. FTIR (KBr, Cm^{-1}); 1405 (SO_3H), 3451 (N-H), 1601 (aromatic C=C), 1521 (H-C=N), 3020 (aromatic C-H). ^{1}H-NMR (D_2O, 400 MHz) δ: 6.74 to 7.68 = Ar-H (m 9H), 11.31 = SO_3H (s 1H), 4.70 = N-H (s 1H), 8.10 = H-C=N (s 1H). ^{13}C-NMR (D_2O, 75 MHz) δ: 115.3, 118.1, 120.1, 128.9, 128.9, 129.2, 129.2, 130.9, 131.1, 133.8, 144.4, 150.6 (Aromatic carbons), 155.9 (C=N). Anal. Calc. for $C_{13}H_{12}N_2O_3S$ (Molecular weight = 276.31 $gmol^{-1}$): S = 11.60, *N* = 10.14, O = 17.37, H = 4.38, C = 56.51% and Found: S = 11.55, *N* = 10.09, O = 17.32, H = 4.35, C = 56.49%.

2.3 | Synthesis of formazan compound 4-(2-(((2-hydroxy-5-nitrophenyl) diazenyl) (phenyl) methylene) hydrazinyl) benzene sulfonic acid (S1)

The formazan compound **(S1)** was synthesized by the azo coupling reaction of diazonium salt **(NAPD)** of 2-amino-4-nitrophenol **(NAP)** and synthesized hydrazone **(BASAH)** (Scheme 1). The diazonium salt **(NAPD)** was prepared by diazotizing of aqueous solution of 0.1 mole of 2-amino-4-nitrophenol **(NAP)** in the presence of $NaNO_2$ (7.4 g) and H_2SO_4 (20 ml) at 10–15 °C. Further, the diazonium salt **(NAPD)** was coupled to coupler agent hydrazone **(BASAH)** in

alkaline media (pH ∼ 8–9) at 0–5 °C. The coupling reaction was monitored by TLC and the reaction was completed within 1 hr. The isolation of the formazan compound **(S1)** was achieved employing salting out process as described by.[9,10] Further, formazan compound **(S1)** was purified by recrystallization process described by.[29,30]

Reddish-brown powder. Yield = 90%. Melting point = 390 °C. λ_{max} in nm (log ε) in ethanol: λ_{max1} = 469 (0.51), λ_{max2} = 339 (0.71), λ_{max3} = 289 (0.31). FTIR (KBr, Cm^{-1}); 1340 (Ar-NO_2), 1415 (SO_3H), 1129 (Ar-OH), 3421 (N-H), 761 (CN=NC), 1615 (aromatic C=C), 1358 (N=N), 1510 (C=N), 3015 (aromatic C-H). ^{1}H-NMR ($CDCl_3$, 400 MHz) δ: 6.49 to 7.59 = Ar-H (m 12H), 11.30 = SO_3H (s 1H), 4.33 = N-H (s 1H), 5.40 = Aromatic-OH (s 1H). ^{13}C-NMR ($CDCl_3$, 75 MHz) δ: 104, 106.5, 118.5, 126.2, 127.1, 128.2, 129.6, 132.3, 135.5, 140.1, 141.3, 147.6, 165.3 (Aromatic carbons), 155.5 (C=N). Anal. Calc. for $C_{19}H_{15}N_5O_6S$ (Molecular weight = 441.417 $gmol^{-1}$): S = 7.26, *N* = 15.87, O = 21.75, H = 3.43, C = 51.70% and Found: S = 7.19, *N* = 15.81, O = 21.69, H = 3.40, C = 51.63%.

2.4 | Synthesis of formazan metal complexes (S2-S6)

The formazan compound **(S1)** is a tridentate ligand and have ability to form metal complexes. Therefore, we further employed formazan compound **(S1)** for the synthesis of different metal complexes following the procedure described by[9,10] with slight modifications. In typical procedure, formazan compound **(S1)** was prepared adopting the methodology described in scheme 1. After, formazan metal complexes **(1:1)** of copper **(S2)**, iron **(S3)**, cobalt **(S5)** and nickel **(S6)** were prepared by the metallization reaction of 0.1 mole of tridentate ligand (formazan compound **S1**) with different metal salts (0.1 mole) such as $CuSO_4.5H_2O$, $FeSO_4.5H_2O$, $CoSO_4.7H_2O$, and $NiCl_2.6H_2O$ respectively at slightly acidic pH ∼ 6.50–6.70 at 65–70 °C. On the other hand, formazan metal complexes **(2:1)** of chromium **(S4)** was synthesized **by** treating 0.1 mole of formazan compound **(S1)** with 0.05 mole of chromium salt $(Cr_3(OH)_2(OOCCH_3)_7$ at slightly acidic pH ∼ 6.70 at elevated temperature 90–100 °C. The metallization reaction was completed within 2–3 hr for (1:1) metal complexes while 3–4 hr for (2:1). The formazan metal complexes **(S2-S6)** was isolated through acidification and salting out methods.[9,10] Therein after, they were purified by recrystallization process described by.[29,30]

2.4.1 | Formazan cu metal complex (S2)

Greyish-black powder. Yield = 91%. Melting point = 420 °C. λ_{max} in nm (log ε) in ethanol: λ_{max1} = 455 (0.45), λ_{max2} = 320 (0.89), λ_{max3} = 285 (0.25). FTIR (KBr, Cm^{-1}); 3390 (O-H), 640 (Cu-O), 1380 (Ar-NO_2), 1285 (SO_3H), 839 (CN=NC), 1589 (aromatic C=C), 1316 (N=N), 1501 (C=N), 3020 (aromatic C-H). ^{1}H-NMR ($CDCl_3$, 400 MHz) δ: 6.79 to 8.60 = Ar-H (m 12H), 11.18 = SO_3H (s 1H). ^{13}C-NMR ($CDCl_3$, 75 MHz) δ: 117.6, 118.8, 126.6, 126.8, 127.1, 128.5, 129.6, 132.1, 132.9, 135.5, 140.1, 141.7, 149.6, 156.6, 159.9 (Aromatic carbons), 155.4 (C=N). Anal. Calc. for $C_{19}H_{19}CuN_5O_9S$ (Molecular weight = 556.932 $gmol^{-1}$): Cu = 11.41, S = 5.76, *N* = 12.57, O = 25.85, H = 3.44, C = 40.97% and Found: Cu = 11.35, S = 5.70, *N* = 12.51, O = 25.80, H = 3.40, C = 40.91%.

2.4.2 | Formazan Fe metal complex (S3)

Reddish-brown powder. Yield = 92%. Melting point = 450 °C. λ_{max} in nm (log ε) in ethanol: λ_{max1} = 449 (0.40), λ_{max2} = 330 (0.99), λ_{max3} = 291 (0.30). FTIR (KBr, Cm^{-1}); 3421 (O-H), 691 (Fe-O), 1358 (Ar-NO_2), 1391 (SO_3H), 828 (CN=NC), 1591 (aromatic C=C), 1435 (N=N), 1531 (C=N), 3030 (aromatic C-H). ^{1}H-NMR ($CDCl_3$, 400 MHz) δ: 6.81 to 8.31 = Ar-H (m 12H), 11.22 = SO_3H (s 1H). ^{13}C-NMR ($CDCl_3$, 75 MHz) δ: 112.3, 117.3, 118.4, 126.2, 128.1, 128.5, 129.6, 132.1, 135.5, 138.1, 140.1, 150.1, 151.3, 160.3, (Aromatic carbons), 155.7 (C=N). Anal. Calc. for $C_{19}H_{19}FeN_5O_9S$ (Molecular weight = 549.292 $gmol^{-1}$): Fe = 10.17, S = 5.84, *N* = 12.75, O = 26.21, H = 3.49, C = 41.54%. Found: Fe = 10.11, S = 5.80, *N* = 12.71, O = 26.20, H = 3.41, C = 41.50%.

2.4.3 | Formazan Cr metal complex (S4)

Greyish-brown powder. Yield = 93%. Melting point = 460 °C. λ_{max} in nm (log ε) in ethanol: λ_{max1} = 471 (0.46), λ_{max2} = 341 (1.01), λ_{max3} = 279 (0.29). FTIR (KBr, Cm^{-1}); 635 (Cr-O), 1351 (Ar-NO_2), 1399 (SO_3H), 849 (CN=NC), 1599 (aromatic C=C), 1465 (N=N), 1516 (C=N), 3035 (aromatic C-H). ^{1}H-NMR ($CDCl_3$, 400 MHz) δ: 6.70 to 8.01 = Ar-H (m 24H), 11.29 = SO_3H (s 2H). ^{13}C-NMR ($CDCl_3$, 75 MHz) δ: 117.6, 118.4, 128.1, 126.4, 127.1, 128.4, 132.6, 133.3, 134.6, 134.8, 136.4, 138.6, 140.0, 141.3, 149.3, 159.9 (Aromatic carbons), 150.3, 155.3 (C=N). Anal. Calc. for $C_{38}H_{26}CrN_{10}O_{12}S_2$ (Molecular weight = 930.799 $gmol^{-1}$): Cr = 5.59, S = 6.89,

N = 15.05, O = 20.63, H = 2.82, C = 49.03% and Found: Cr = 5.55, S = 6.80, *N* = 14.99, O = 20.60, H = 2.80, C = 49.01%.

2.4.4 | Formazan co metal complex (S5)

Dark-brown powder. Yield = 90%. Melting point = 410 °C. λ_{max} in nm (log ε) in ethanol: λ_{max1} = 480 (0.48), λ_{max2} = 349 (1.20), λ_{max3} = 281 (0.33). FTIR (KBr, Cm^{-1}); 3345 (O-H), 641 (Co-O), 1315 (Ar-NO_2), 1231 (SO_3H), 799 (CN=NC), 1599 (aromatic C=C), 1324 (N=N), 1501 (C=N), 3010 (aromatic C-H). ^{1}H-NMR ($CDCl_3$, 400 MHz) δ: 6.89 to 8.67 = Ar-H (m 12H), 11.21 = SO_3H (s 1H). ^{13}C-NMR ($CDCl_3$, 75 MHz) δ: 112.3, 117.3, 118.4, 126.2, 128.1, 128.5, 129.6, 132.2, 135.5, 138.1, 140.4, 150.1, 151.3, 160.1 (Aromatic carbons), 155.9 (C=N). Anal. Calc. for $C_{19}H_{19}CoN_5O_9S$ (Molecular weight = 552.380 $gmol^{-1}$): Co = 10.67, S = 5.68, *N* = 12.68, O = 26.07, H = 3.47, C = 41.31% and Found: Co = 10.60, S = 5.63, *N* = 12.59, O = 26.01, H = 3.39, C = 41.30%.

2.4.5 | Formazan Ni metal complex (S6)

Greenish-brown powder. Yield = 91%. Melting point = 435 °C. λ_{max} in nm (log ε) in ethanol: λ_{max1} = 475 (0.41), λ_{max2} = 343 (1.30), λ_{max3} = 291 (0.27). FTIR (KBr, Cm^{-1}); 3446 (O-H), 641 (Ni-O), 1338 (Ar-NO_2), 1315 (SO_3H), 861 (CN=NC), 1609 (aromatic C=C), 1401 (N=N), 1499 (C=N), 3040 (aromatic C-H). ^{1}H-NMR ($CDCl_3$, 400 MHz) δ: 6.88 to 8.71 = Ar-H (m 12H), 11.30 = SO_3H (s 1H). ^{13}C-NMR ($CDCl_3$, 75 MHz) δ: 112.6, 117.9, 118.4, 126.2, 128.1, 128.5, 129.6, 132.3, 135.5, 138.4, 140.1, 150.9, 151.3, 160.1 (Aromatic carbons), 155.3 (C=N). Anal. Calc. for $C_{19}H_{19}NiN_5O_9S$ (Molecular weight = 552.140 $gmol^{-1}$): Ni = 10.63, S = 5.81, *N* = 12.68, O = 26.08, H = 3.47, C = 41.33% and Found: Ni = 10.60, S = 5.80, *N* = 12.60, O = 26.01, H = 3.40, C = 41.27%.

2.5 | Antioxidant activity

The synthesized formazan compounds **(S1-S6)** were screened for their antioxidant propensity employing a modified-protocol based on Brand–William's procedure.[39–43] In a typical procedure, the 20 µl of methanolic suspensions of each synthesized formazan compounds **(S1-S6)** were mingled with 180 µl of 1 mM methanolic DPPH solution. The different concentrations of each synthesized formazan compounds **(S1-S6)** (75, 150, 250, 500 and 1000 µg/ml) were selected. Standard antioxidant "Vitamin C" was employed as a positive control. The reaction mixture was incubated in dark condition for 30 min at room temperature (25–30 °C),[44,45] and the changes in color was recorded by measuring absorption maxima (λ_{max}) at 517 nm through an ELISA reader. The free radical-scavenging activity was calculated as percentage inhibition of DPPH employing following equation.

$$\text{Percentage inhibition of DPPH} = \left[\left(A_{\text{control}} - A_{\text{sample}}\right) / A_{\text{control}}\right] \times 100.$$

where A_{sample} is the absorbance of the DPPH solution with synthesized non-metal and complex formazans (**S1-S6**) while Acontrol is the absorbance of the DPPH solution without synthesized formazan compounds **(S1-S6)**. The experiments were performed in triplicates with a mean ± standard error.

2.6 | Antibacterial activity

The synthesized metal complex formazans **(S1-S6)** were scrutinized for their antibacterial propensity against different bacteriological strains such as *Staphylococcus epidermidis* (ATCC 12228), *Bacillus cereus* (ATCC 11778), *Klebsiella pneumoniae* (ATCC BAA-1705™) *Pseudomonas aeruginosa* (ATCC 15442).[46–49] These bacteriological strains were acquired from Pakistan Chemical Scientific Industrial Research (PCSIR) laboratories complex, Lahore, Pakistan. The bactericidal propensity of synthesized metal complex formazans **(S1-S6)** was deliberated on agar plates by well-known agar well diffusion method as described by.[50–52] For each type of microbial species, the streptomycin and neomycin were employed as a standard antibiotic drug (positive control).[53–55]

2.7 | Antimycotic activity

The antimycotic propensity of the synthesized metal complex formazans **(S1-S6)** were evaluated against different mycological strains such as *Trichophyton mentagrophytes* (ATCC 9533), *Candida albicans* (ATCC 10231), *Aspergillus niger* (ATCC 16404), *Saccharomyces cerevisiae* (ATCC 9763) and *Candida glabrata* (ATCC 90030) adopting the standard protocol described by.[56,57] The employed fungal microorganisms were acquired from the microbiology laboratory of University of Veterinary and Animal Science Lahore, Pakistan. Terbinafine and Fluconazole were served as standard antimycotic

drugs (positive control) for the comparative study of antimycotic propensity against different fungal strains.

2.8 | MTT cell proliferation assay

By employing 3–(4, 5-dimethyl-2-thiazolyl)-2, 5-diphenyl-2H tetrazolium bromide (MTT) (Life Technologies, Eugene, OR) assay, the cell viability of human breast carcinoma (MCF-7) cell line treated by synthesized metal complex formazans **(S1-S6)** were assessed. The human breast carcinoma (MCF-7) cell line at 37 °C in a moistened thermosphere comprising of 95% air and 5% CO_2 was cultured in Dulbecco's modified Eagles medium (DMEM) (Gibco-BRL, Grand Island, NY) subsequently they were seeded at a density of 1×10^4 per well in a 96-well plate (Corning Costar, Lowell, NY, USA). Used Dulbecco's modified Eagles medium (DMEM) was supplemented with 1% penicillin/streptomycin (P/S) and 10% foetal bovine serum (FBS). Afterwards, the wells containing cultured human breast carcinoma (MCF-7) cell line in a 96-well plate were subjected to treat with different concentrations (1, 10, 20, 30, 40 and 50 μg/ml) of standard (Doxorubicin), and synthesized formazans **(S1-S6)** at 37 °C for 48 hr at 90% confluency. Subsequently, the wells were further incubated at 37 °C for 4 hr after the addition of 10 μl of MTT (5 mg/ml) in PBS solution. Moreover, to dissolve the unsolvable formazan crystals into the colored solution, 100 μl of dimethyl sulphoxide (DMSO) was added in each well. An enzyme-linked immunesorbent assay (ELISA) reader (Bio-Tek Instruments, Inc., Vinooski, VT, USA) was employed to measure the absorption maxima of reaction mixture in each well. Results were expressed as the percentage of the control (without compound set at 100%). The percentage of cell survival was calculated as OD value of cells treated with the test compound−OD value of culture medium/(OD value of control cell−OD value of culture medium) × 100%. The experiment was performed in triplicates with a mean ± standard error.

2.9 | Molecular docking studies

Computational biology is the ultimate source of attraction in drug designing due to its low coast and quick results leading a new pathway in drug discovery. For better drug designing and prediction, molecular docking is a great tool and success that not only mention the active site for the reaction of drug but also its binding affinity along with other biological effects. After the evolution of synthesized formazan compounds **(S1-S6)** for their cytotoxic potential in *vitro* on human breast carcinoma (MCF-7) cell line, they were further screened for docking studies to know on what level and how they can combine with breast cancer causing protein (The human estrogen receptor).

2.9.1 | Recuperate of protein and ligand formation

For docking studies of synthesized formazan compounds **(S1-S6)** with the breast carcinoma cells, the human estrogen receptor protein was used as three dimensional structure and was taken from protein data bank with PDB ID: 2IOK and resolution of 2.4 Å.[58] The excluding entities like water was removed in Accelrys discovery studio visualizer.[59] On the basis of experiment and literature, synthesized formazan compounds **(S1-S6)** were chosen and made in chem draw for the docking process. The Doxorubicin was used as standard ligand for further analysis due to its reviews as better anticancer drug. It was taken from PubChem with CID: 31703.[60] All the ligands were made in.sdf file, which was later converted into.pdb file using discovery studio visualizer.

2.9.2 | Docking

In order to find out the action of ligands **(S1-S6)** over the protein, docking was executed and the results with different ligands were compared. The process was executed using autodock and vina autodock and later analyzed by using discovery studio resulting 3d representation. Autodock was also used for charge addition both in estrogen receptor protein and the ligands. The protein receptor was added with kollman charge while the ligands had gesteiger charges with the minimization of torsions. Thus, the ligands and receptor were converted into.pdbqt format after the above operations.[61,62]

2.9.3 | Physico-chemical properties analysis

Drug designing is resulted by a number of experimental and computational processes where physico-chemical properties play an important role as they indicates the drug capability to interact with the biological process along with the environmental process and the physical hazards. Here the physico-chemical properties include molecular weight, total surface area, polar surface area, druglikeness, clogP and clogS. The druglikeness follows Lipinski rule of five for the drug analysis. All the properties were found out using Data warrior.[63]

2.10 | Computational methods

All computations were carried out using Gaussian 09 W software package.[64] The molecular geometry for the studied compounds were fully optimized using Density functional theory B3LYP method,[65–67] by implementing LANL2DZ basis set for Cu, Fe, Cr, Co and Ni-atoms[68,69] and 6–31 + G(d,p)[70] basis set for the rest of atoms. No symmetry constrains were applied during the geometry optimization.[71,72] NBO calculations have been performed at the same level of calculation by using NBO 3.1 program as implemented in the Gaussian 09 W software package. The optimized structure was visualized using Chemcraft version 1.6 package[73] and GaussView version 5.0.9.[74] Furthermore, the Multiwfn v3.7 software program was used[75] in order to compute quantum chemical descriptors from CDFT point of view.

3 | RESULTS AND DISCUSSION

3.1 | Antioxidant activity

The newly synthesized formazan compounds **(S1-S6)** were scrutinized for the assessment of their antioxidant potential by DPPH free radical scavenging assay and their antioxidant results in terms of percentage inhibition of DPPH are presented in Figure S1. It has been anticipated from the results that maximum and superior antioxidant propensity in terms of percentage inhibition of DPPH free radical (73.5%, 80%, 83%, 86%, 90%) was unveiled by all the concentrations (75 μg/ml, 150 μg/ml, 250 μg/ml, 500 μg/ml, 1000 μg/ml) of formazan compound **(S1)** respectively, which were analogous to the employed standard antioxidant "Ascorbic acid". While the formazan compounds **(S2, S3, S5, S6)** demonstrated the moderate to good antioxidant propensity by scavenging the DPPH free radical as presented in Figure S1. The formazan compound **(S4)** exhibited least antioxidant propensity. Further, results were also attributed concentration dependent antioxidant activity as increasing concentration of the formazan compounds **(S1-S6)** exhibited effective and enhanced percentage inhibition of DPPH free radical. Literature data demonstrates that antioxidants combine with a stable free radical DPPH to transform it to 2,2-diphenyl-1- picryl hydrazine which results in the decoloration of DPPH. Therefore, the scavenging aptitudes of the tested compounds were determined from the degree of decoloration of DPPH (more degree of coloration, more will be scavenging and vice versa).

3.2 | Antibacterial activity

The antibacterial propensity of the synthesized formazan compounds **(S1-S6)** was executed against *Staphylococcus epidermidis*, *Bacillus cereus* (Gram-positive bacteria), *Klebsiella pneumoniae* and *Pseudomonas aeruginosa* (Gram-negative bacteria) and their outcomes are shown in Figure S2 in the form of their zone of inhibitions values (ZOIs) while their results of minimum inhibitory concentration values (MICs) in μg/mL are presented in Table S1. ZOIs results were demonstrated that the synthesized formazan compound **(S1)** was found to exhibit least antibacterial propensity by presenting minimum ZOIs values (21 ± 0.08 mm, 19 ± 0.02 mm, 15 ± 0.04 mm, 17 ± 0.08 mm) against *Staphylococcus epidermidis*, *Bacillus cereus, Klebsiella pneumoniae* and *Pseudomonas aeruginosa* respectively compared to metal complex formazan compounds (**S2-S6**) and employed standard drugs. On the other hand, the synthesized formazan compounds (**S2, S3, S5 and S6**) were demonstrated the moderate to good antibacterial propensity (Figure S2). Moreover, substantial and enhanced antibacterial propensity was exhibited by the formazan compound **(S4)** with the maximum ZOIs values (33 ± 0.04 mm, 32 ± 0.09 mm, 26 ± 0.01 mm, 27 ± 0.05 mm) against of *S. epidermidis*, *B. cereus, K. pneumoniae* and *P. aeruginosa* respectively in comparison to metal complex formazan compounds (**S2**, **S3**, **S5** and **S6**) and standard drugs. It has been also anticipated from the MICs results that formazan compound **(S4)** were found to unveil the similar MICs results to that of standard antibiotics drugs (streptomycin and neomycin) while the other formazan compounds **(S1, S2, S3, S5, S6)** were found to exhibit least MICs results (Table S1). The fact due to which formazan compounds **(S1-S6)** presented moderate to noteworthy and substantial antibacterial propensity was the structural moiety i.e. substitution of electron-withdrawing group (-SO_3H and -NO_2) on the *para* position of benzene ring (Scheme 1), which enable them to unveil significant and effective bactericidal potential. Moreover, literature survey also exposes that antibacterial propensity depends on the position and existence of functional groups within the molecular structure[9,10,48] and electron-withdrawing groups (–NO_2, –CN, -SO_3H, –CHO, –C=O) are responsible to upsurge the antibacterial propensity of the molecule compared to electron-donating groups ($–O^-$, –NH_2, –NHR, –OR, –NHCOR). Furthermore, *ortho* and *para* positions are more favorable to augment the bactericidal potential than *meta* position as more stabilization of the molecular structure can be achieved when electron-withdrawing groups positioned on these two positions of benzene ring.[9,10] Henceforth, it was ostensible and

established from the outcomes of MICs and ZOIs that the nature of formazan compounds **(S1-S6)** is bacteriostatic as well as bactericidal, which empower them to demonstrate substantial antibacterial propensity against Gram-positive and Gram- negative bacteria.

3.3 | Antimycotic activity

The antimycotic propensity of the synthesized formazan compounds **(S1-S6)** was evaluated against *Trichophyton mentagrophytes*, *Candida albicans*, *Aspergillus niger*, *Saccharomyces* cerevisiae, and *Candida glabrata*. The outcomes of antimycotic propensity in the form of minimum inhibitory concentration (MICs in μg/mL) and zone of inhibitions values (ZOIs) are manifested in Figure S3 and S4 respectively. ZOIs results were demonstrated that significant and superior antimycotic propensity was unveiled by the formazan compound **(S4)** with the maximum ZOIs values (33 ± 0.04 mm, 29 ± 0.09 mm, 39 ± 0.01 mm, 36 ± 0.05 mm, 30 ± 0.05 mm) against *T. mentagrophytes*, *C. albicans*, *A. niger*, *S.* cerevisiae and *C. glabrata* respectively in contrast to formazan compounds (**S2**, **S3**, **S5** and **S6**) and standard drugs (Terbinafine and Fluconazole). While the synthesized formazan compound (S1) against each fungal strains were demonstrated the least antimycotic propensity in contrast to formazan compounds (**S2-S6**) and employed standard drugs. On the other hand, the synthesized formazan compounds (**S2, S3, S5 and S6**) were demonstrated the moderate to good antimycotic propensity. Moreover, It has been also anticipated from the MICs results that formazan compound **(S4)** were found to unveil the similar MICs results to that of standard antibiotics drugs while the other formazan compounds **(S1, S2, S3, S5, S6)** were found to exhibit least MICs results (Figure S3). Hence, it was apparent and proven from the outcomes of MICs and ZOIs that formazan compounds **(S1-S6)** are fungicidal in nature, which endow them to demonstrate substantial antifungal propensity against employed fungal strains.

3.4 | MTT cell proliferation assay

The human breast carcinoma (MCF-7) cell lines as in *vitro* models for cancerous cells were employed to determine the cytotoxicity potential of the formazan compounds **(S1-S6)** and their cytotoxicity results are manifested in Figure S5. The cytotoxicity potential of the formazan compounds **(S1-S6)** is profoundly influenced by the substitution of electron-donating groups (-OH, $-NH_2$, OCH_3, $-CH_3$) in their molecular structures. It has been anticipated from the cytotoxicity results that human breast carcinoma (MCF-7) cell line treated with the formazan compounds **(S1-S6)** was found to exhibit concentration dependent anticancer propensity. The maximum cytotoxic effect (49%, 55%, 62%, 74%, 79%, 84%) on human breast carcinoma (MCF-7) cell line was experimented with the different concentrations (50 μg/ml, 40 μg/ml, 30 μg/ml, 20 μg/ml, 10 μg/ml, 1 μg/ml) of formazan compound **(S1)** respectively in contrast to other formazan compounds **(S2, S3, S4, S5, S6)** but was comparable to that of employed standard anticancer drug "Doxorubicin". Moreover, the other formazan compounds **(S2, S3, S5, S6)** along with their different concentrations were demonstrated the moderate level cytotoxic effect on human breast carcinoma (MCF-7) cell line however, among all, the least cytotoxicity on breast carcinoma cells was perceived by the formazan compound **(S4)** as presented in Figure S5. From these findings, we assumed that more percentage cytotoxic effect results in decreasing the cell viability and vice versa. According to the results of MTT cell proliferation assay, formazan compounds have possess the capability to impede the breast cancer cells proliferation. Conclusively, it was evident and confirmed from the cytotoxicity results that formazan compounds **(S1-S6)** have potential towards to act as anticancer.

3.5 | Docking studies of the synthesized formazan compounds (S1-S6)

The docking studies indicates the binding of human estrogen receptor with different ligands **(S1-S6)** along with the doxorubicin, which is the standard drug for the breast cancer to analyze the protein binding activity computationally. The docking process provided the binding affinity and inhibitory constant which indicated the almost all the ligands had good values except ligand (formazan compound **S4**) (Table S2). The K_i value of all **(S1, S2, S3, S5, S6)** except the already mentioned **(S4)** are more better than the standard doxorubicin indicating better binding of ligands at active site of protein and thus indicating better IC_{50} value that plays a better role mode of action of drug in body. The less the K_i value, the better IC_{50} value resulting in better drug activity.[58–61] As far as bonding is concerned, the presence of benzene rings and amine groups provided the pi bond in high frequency while the hydrogen bonds are less in number though present. The binding sites in ligands **(S1-S6)** revealed some common residues to bind with the receptor protein which are Glu_{323}, Pro_{324}, Ile_{326}, Met_{343}, Leu_{346}, Thr_{347}, Leu_{349}, Ala_{350}, Asp_{351}, His_{373}, His_{377}, Glu_{380}, Trp_{383}, Leu_{387}, Trp_{393}, Arg_{394}, Glu_{397}, Phe_{404}, Met_{421}, Ile_{424}, Phe_{445},

Arg_{515}, Ser_{516}, Ser_{518}, Asn_{519}, Met_{522}, Glu_{523}, Leu_{525}, Tyr_{526}, Pro_{535}, Leu_{536} and Tyr_{537} (Figures S6-S11).

3.6 | Physico-chemical properties analysis

The physico-chemical properties were analyzed revealing molecular weight, total surface area, polar surface area, druglikeness, clogP and clogS of different ligands (Table 1). The most important Lipinski rule of five for druglikeness indicates that the molecular weight for the drug must be greater than 500 Da and calculated logP must be greater than 5.[58–60] The given results indicated that the most ligands were having more than 500 Da molecular weight except ligand **(S1)** while the logP value is not in range for all ligands even for the standard drug. The ratio of total surface area and polar surface area revealed almost all the ligands **(S1-S6)** have mostly polar surface area making them almost the polar ligand. As far as calculated druglikeness is concerned the standard drug has the positive value while all the other ligands **(S1-S6)** were having negative values for druglikeness. The values for logS is almost in between −6.23 to 0.907 while the standard range of logS is between −2 to −5. Thus, only ligand **(**formazan compound, **S1)** and doxorubicin are in the standard range.[61]

3.7 | Density functional theory (DFT) studies

3.7.1 | Structural properties

The optimized geometrical parameters (bond lengths, bond angles and dihedral angles), natural charges on active centers, reactivity descriptors, molecular electrostatic potential maps and energetic of the ground state for the studied complexes were computed and analyzed. From the elemental analysis and spectroscopic data, metal ions coordinated to the ligand via N and O atoms forming the complexes. One ligand moiety used in the coordination with Cu (II) (**S2**), Fe (II) (**S3**), Co (III) (**S5**) and Ni (II) (**S6**) forming $[ML(H_2O)_3]$ complexes and two ligand moiety in case of Cr (III) (**S4**) forming $[CrL_2]$.

3.7.2 | Geometry of the complexes

Tables 2 and Figure 1 present the optimized geometry, numbering system, vector of the dipole moment, energetic, bond lengths, bond angles and dihedral angles of all metal complexes studied in this work. In Cu (II), Fe (II), Co (III), Ni (II) and Cr (III) complexes, the metal ion coordinates with O7 and N14 from the ligand to form a five-member ring with the sequences O7,C6,C1,N14 there are another chelation with N14 and N18 from a six-member ring with the sequences N14,N15,C16,N17,N18 and three water molecule in all complexes except Cr (III) which contained two ligand molecules to form two five- and two six-membered rings with sequences O7,C6,C1, N14, O52,C51,C46,N59, and N14,N15,C16,N17,N18, N59,N60,C61,N62,N63 respectively. Therefore, form regular octahedral geometry is expected for all the studied complexes except in case of Cu (II) distortion of octahedral geometry. Most M-N and M-O bonds show elongation upon chelation. The length of the coordinate covalent bonds between metal and ligand site, i.e. M-N and M-O, are too long compared to the typical MX bond lengths.[76] The too long M-O and M-N bonds in the studied complexes mean that the ionic character of these bonds is small which is vary between 1.89 to 2.07 Å (Table 2). The calculated values of bond angles between metal ion and binding sites (Tables 2) C6O7M, O7MN14, O7MO49(O52), O7MO49(N59) and N14MN18 vary between 80 and 112 degree, which compare nicely with the experimental data as obtained from X-ray analysis for OH complexes,[72] which indicate a regular octahedral geometry is expected for all the studied complexes except in case of Cu (II) distortion of octahedral geometry. The

TABLE 1 The physico-chemical properties analysis of formazan compounds **(S1-S6)** towards human estrogen protein receptor for drug designing

Formazan Compounds	Molecular weight	Total surface area	Polar surface area	Drug likeness	clogP	clogS
S1	442.431	317.58	176.92	−13.682	−1.1844	−3.131
S2	554.337	339.96	209.36	−6.3567	−1.3126	0.745
S3	562.038	339.96	209.36	−4.5067	−1.3126	0.745
S4	935.850	625.56	331.02	−25.31	−2.2736	−6.235
S5	557.158	339.96	209.36	−3.8167	−1.3126	0.745
S6	557.425	339.96	209.36	−3.9367	−1.3126	0.745

Values are mean ± SD triplicate assays.

TABLE 2 The selected bond length (Å), bond angles and dihedral angles, (degree) of H_2L (**S1**), Cu (II) (**S2**), Fe (II) (**S3**), Cr (II) (**S4**), Co (III) (**S5**) and Ni (II) (**S6**) complexes B3LYP/GENECP level of theory

	H_2L (S1)		Cu (II) (S2)	Fe (II) (S3)	Co (III) (S5)	Ni (II) (S6)	Cr (III) (S4)	
R(C1-C6)	1.42		1.44	1.43	1.44	1.44	1.44	
R(C1-N14)	1.41		1.40	1.42	1.39	1.41	1.40	
R(C6-O7)	1.36		1.31	1.32	1.30	1.31	1.31	
R(O7-M45)	R(−,H45)	0.97	1.99	1.96	1.93	2.03	1.20	
R(N14-N15)	1.277		1.27	1.29	1.29	1.28	1.30	
R(N14-M45)	R(−,H46)	1.03	1.98	1.87	1.89	2.01	2.02	
R(C16-N17)	1.32		1.33	1.34	1.37	1.34	1.32	
R(N17-N18)	1.32		1.30	1.32	1.29	1.31	1.31	
R(N18-C19)	1.39		1.41	1.42	1.43	1.42	1.41	
R(N18-M45)	R(−,H46)	1.03	1.97	1.89	1.94	2.04	2.07	
R(M45-O46)			2.64	2.36	2.32	2.17	R(−,O52)	1.20
R(M45-O49)			4.67	4.62	2.37	2.22	R(−,N59)	2.02
R(M45-O52)			2.10	2.07	2.05	2.19	R(−,N63)	2.07
A(C1-C6-O7)	117.7		120.0	118.0	118.2	120.1	118.6	
A(C6-O7-M45)	109.9		110.9	111.0	111.0	111.1	112.7	
A(C1-N14-M45)			111.0	112.7	111.8	111.3	112.1	
A(N15-N14-M45)			129.6	130.3	130.4	130.6	127.8	
A(N17-N18-M45)			126.4	127.4	126.2	124.7	119.3	
A(O7-M45-N14)			84.2	85.3	85.7	83.1	79.5	
A(O7-M45-O46)			71.7	77.4	87.2	87.0	A(−,-,O52)	180.0
A(O7-M45-O49)			103.1	99.7	87.6	86.8	A(−,-,N59)	100.5
A(O7-M45-O52)			85.8	81.6	82.7	79.6	A(−,-,N63)	83.4
A(N14-M45-N18)			88.3	90.8	90.8	88.8	76.2	
A(N18-M45-O46)			103.7	83.9	92.8	93.1	A(−,-,O52)	83.4
A(N18-M45-O49)			87.4	102.1	100.9	109.2	A(−,-,N59)	103.8
A(N18-M45-O52)			105.2	91.5	85.8	85.5	A(−,-,N63)	180.0
D(N-14-C1-C6-C5)	179.9		178.5	179.2	178.9	179.5	176.5	
D(N14-C1-C6-O7)	−0.02		−2.2	−1.2	−0.4	−0.3	1.5	
D(C6-C1-N14-N15)	−179.9		−178.9	−179.0	−177.4	−177.1	155.2	
D(C6-O7-M45-N14)			−0.6	0.3	4.1	3.6	−20.8	
D(C6-O7-M45-O46)			−118.5	−111.0	−92.6	−93.0	D(−,-,-,O52)	−22.2
D(C6-O7-M45-O49)			155.6	151.0	99.2	98.1	D(−,-,-,N59)	159.3
D(C6-O7-M45-O52)			147.7	155.6	−178.7	−178.9	D(−,-,-,N63)	84.7
D(M45-N14-N15-C16)				0.9	1.5	2.0	22.5	
D(C1-N14-M45-N18)				178.6	175.5	177.0	121.1	
D(N15-N14-M45-N18)			−8.6	−3.2	−6.8	−5.5	−52.2	
D(N15-N14-M45-O46)			−112.9	−107.9	−99.9	−99.9	D(−,-,-,O52)	28.3
D(N15-N14-M45-O49)			71.4	75.7	86.1	87.5	D(−,-,-,N59)	37.6
D(N15-N14-M45-O52)			107.1				D(−,-,-,N63)	127.8

Values are mean ± SD triplicate assays.

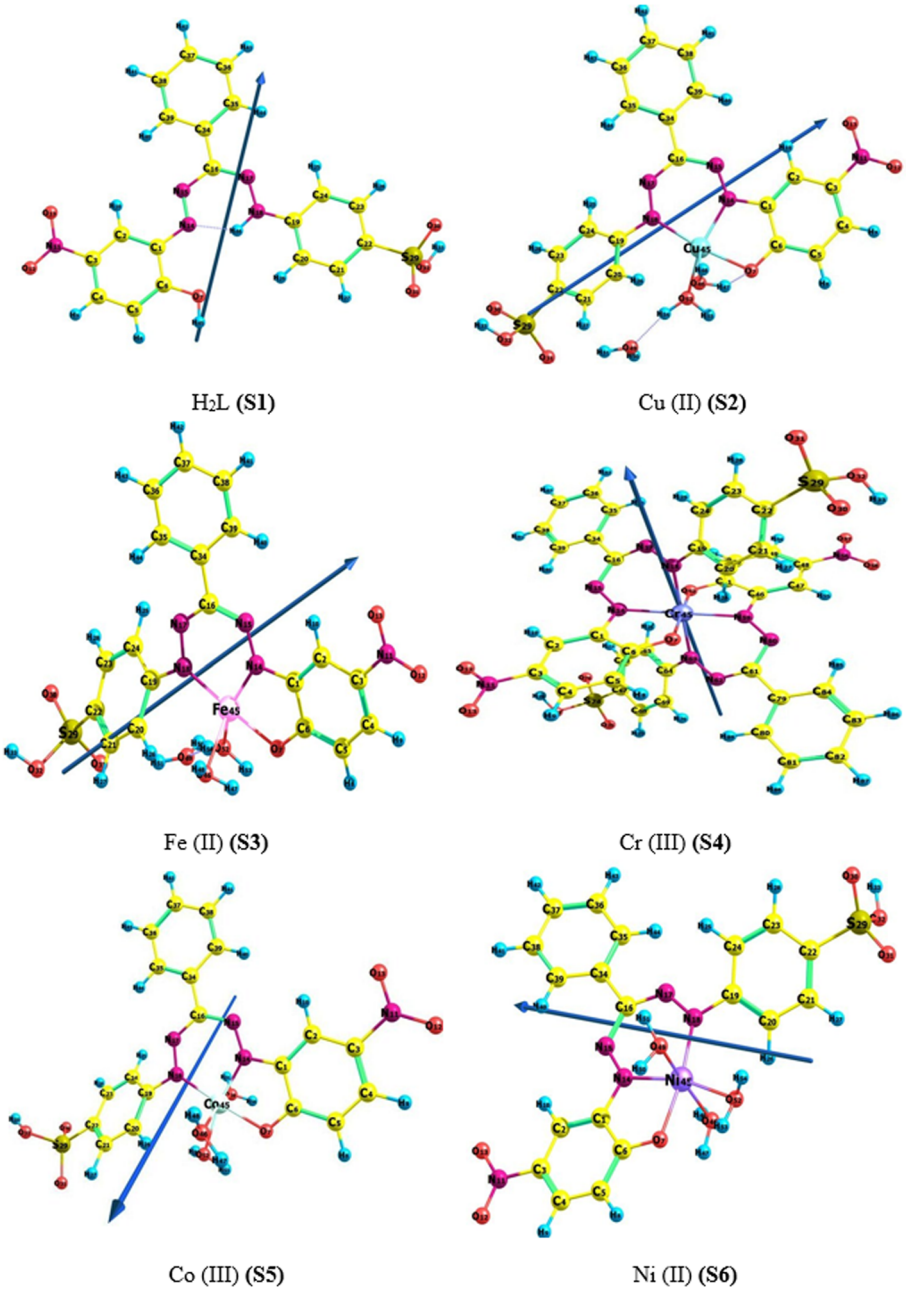

FIGURE 1 The optimized geometry, numbering system, vector of dipole moment of H_2L (**S1**), Cu (III) (**S2**), Fe (II) (**S3**), Cr (III) (**S4**), Co (III) (**S5**) and Ni (II) (**S6**) complexes using B3LYP/GENECP level of calculation

computed values of dihedral angles around metal ion represent in Table 2, i.e. N14C1C6C5, C6C1N14N15, C6O7MN14, MN14N15N18 and C1N14MN18, are close from 0 or 180° which indicate that the metal ion is in the same molecular plane of the ligand except Cr-molecule out of plane with perfect octahedral structure and other coordination with water are close to 95° except in case of Cu (II) complex there are large deviation from regular octahedral structure.

3.7.3 | Natural charges and natural population

The natural population analysis performed on the electronic structures of the studied complexes clearly describes the distribution of electrons in various subshells of their atomic orbits. The natural charges on the coordinating sites in the core, valence and Rydberg subshells and natural electronic configuration of the metal in the studied complexes are presented in Tables 3 and S3. The most electronegative centers are accumulated on O7, N14, N18, O46, O49 and O52. These electronegative atoms have a tendency to donate electrons. Whereas, the most electropositive atoms are Cu, Fe, Co, Ni and Cr have a tendency to accept electrons and incase of Cr the most electronegative centers are localized on O7, N14, N18, O52, N59 and N63 because Cr coordinated with two ligand molecules. The central metal ion in the Cu, Fe, Co, Ni and Cr complexes received 1.11e, 1.23e, 2.09e, 1.31e and 2.6e from the donating active sites of the

TABLE 3 Natural charge on coordinated atoms of H_2L (**S1**), Cu (II) (**S2**), Fe (II) (**S3**), Cr (III) (**S4**), Co (III) (**S5**) and Ni (II) (**S6**) complexes using B3LYP/GENECP level of theory

Atom	H_2L (S1)	Cu (II) (S2)	Fe (II) (S3)	Co (III) (S5)	Ni (II) (S6)	Cr (III) (S4)	
O7	−0.679	−0.75	−0.718	−0.656	−0.771	−0.599	
N14	−0.215	−0.257	−0.232	−0.154	−0.29	−0.173	
N17	−0.236	−0.208	−0.238	−0.208	−0.227	−0.218	
O46		−0.992	−0.976	−0.97	−0.952	**O52**	−0.599
O49		−1.012	−1.038	−0.977	−0.962	**N59**	−0.174
O52		−1.006	−0.985	−0.928	−0.967	**N62**	−0.218

Values are mean ± SD triplicate assays.

ligands with d-orbit electronic configuration $3d^{9.44}$, $3d^{6.63}$, $3d^{8.36}$, $3d^{7.65}$, $3d^{4.88}$ from the active sites of the ligands respectively.

3.7.4 | Frontier molecular orbitals (FMOs) analysis

The values of the calculated quantum chemical parameters such as the energy of the highest occupied molecular orbital (E_{HOMO}), energy of the lowest unoccupied molecular orbital (E_{LUMO}), energy gap (ΔE_{gap}), ionization energy (I), electron affinity (A)[77,78] are presented in Table 4. The value of HOMO energy determines the ability of electron to be donated. When the value of E_{HOMO} is high, it indicates the ease of donating electron to the unoccupied orbital of the receptor molecule. When the value of E_{LUMO} is small, this means that it has a small resistance to accept electrons so it will be more able to accept electron. The HOMO and LUMO energy values are related to the ionization potential ($I = -E_{HOMO}$) and electron affinities ($A = -E_{LUMO}$). The difference between HOMO and LUMO energy values gives the HOMO-LUMO energy gap. The compound **S3** showed highest energy gap ($\Delta E_{gap} = 2.64$) which indicates its higher stability and less reactivity. The molecule that have the lowest energy gap is the molecule **S5** ($\Delta E_{gap} = 2.14$ eV) indicating its lowest stability and high reactivity and other derivative gradient decreasing order as **S2** < **S4** < **S6** < **S1**. The two properties like I (potential ionization) and A (electron affinity) are so important, the determination of these two properties allow us to calculate the global reactivity descriptors. These two parameters are related to the one-electron orbital energies of the HOMO and LUMO respectively. The more I is lower, the molecule will be the better electron donor. The more A is larger the molecule will be the better electron acceptor From Table 4, **S5** have the highest values of both I and A verses other derivatives with order of I as **S1** > **S2** > **S3** > **S6** > **S4** in case A, order is **S2** > **S1** > **S6** > **S3** > **S4**. From Figure 2, it is cleared that the dispersion of isodensities of HOMOs and LUMOs is almost similar in all the compounds, which dispersed on the phenyl rings of ligand and the coordination active centers.

3.7.5 | Global reactivity descriptors

Chemical reactivity can be simply defined as the tendency of a chemical matter to undergo chemical reaction with another chemical matter. It is well-known that the understanding of the nature of chemical interactions and the prediction of chemical reactivity of atoms, ions or

TABLE 4 Molecular orbital energies and other properties of synthesized derivatives **(S1-S6)**

Compounds	E_{HOMO} (eV)	E_{LUMO} (eV)	Energy gap ΔE (eV)	Ionization Potential, *I* (eV)	Electron Affinity, *A* (eV)	Dipole moment debye (D)
H_2L **(S1)**	−6.13	−3.62	2.51	6.13	3.62	2.76
Cu (II) **(S2)**	−5.90	−3.76	2.14	5.90	3.76	7.00
Fe (II) **(S3)**	−5.77	−3.13	2.64	5.77	3.13	8.19
Cr (III) **(S4)**	−3.72	−1.34	2.38	3.72	1.34	0.00
Co (III) **(S5)**	−9.62	−7.78	1.85	9.62	7.78	1.85
Ni (II) **(S6)**	−5.74	−3.35	2.40	5.74	3.35	2.92

Values are mean ± SD triplicate assays.

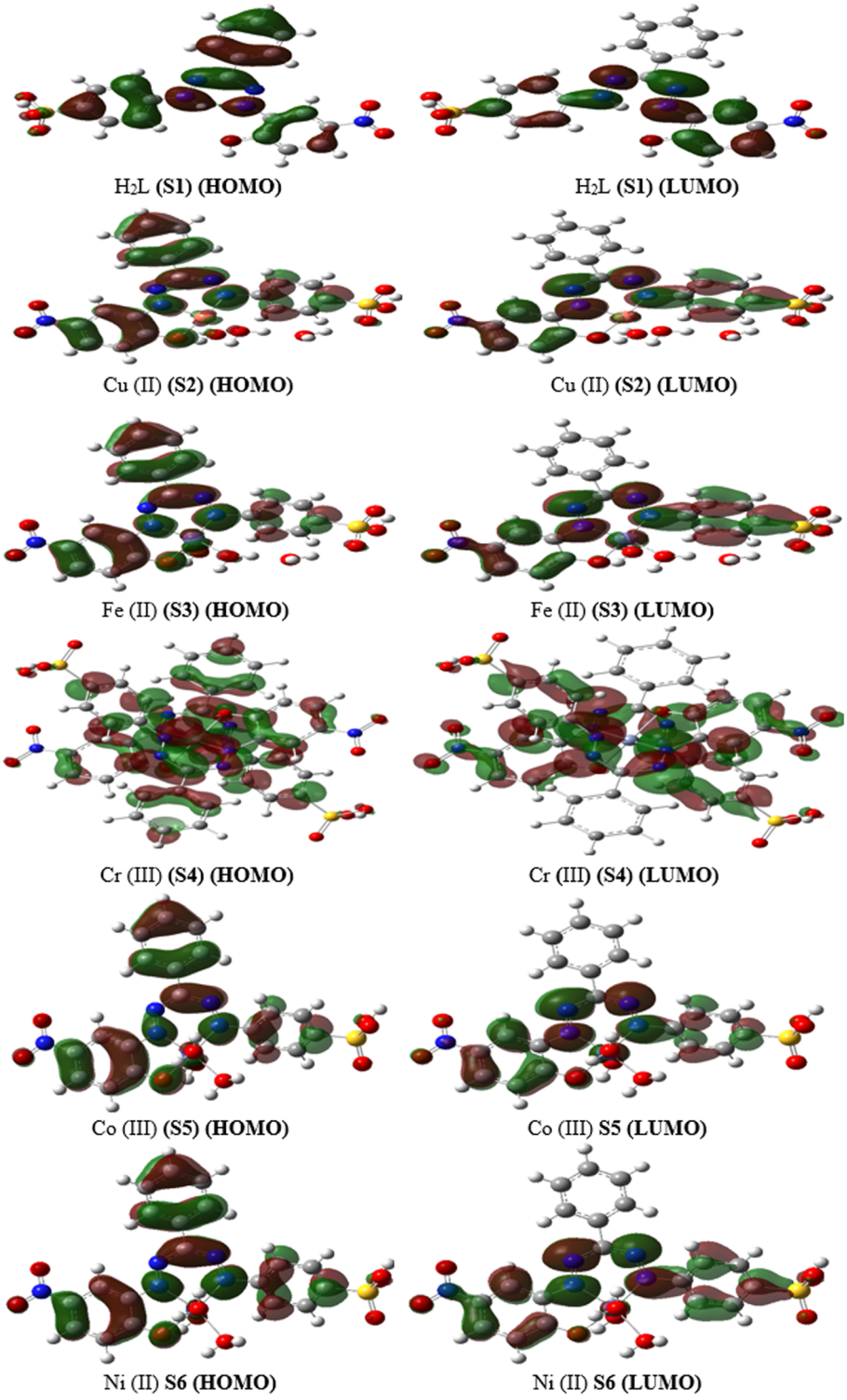

FIGURE 2 Frontier molecular orbitals of the newly synthesized formazan compounds (**S1-S6)**

molecules are some of the challenging issues in chemistry, which are important to explain the reactivity of synthesized formazan compounds **(S1-S6)**. In the CDFT, quantum chemical descriptors like chemical hardness (η), electronic chemical potential (μ), and electronegativity (χ) are usually considered. μ and η are defined as the first derivative of the electronic energy and chemical potential with respect to the electron number (N) at constant external potential, v(r), respectively.[79,80]

$$\mu = \left(\frac{\partial E}{\partial N}\right)_{v(r)} \quad (1)$$

$$\eta = \frac{1}{2}\left(\frac{\partial^2 E}{\partial N^2}\right)_{v(r)} = \frac{1}{2}\left(\frac{\partial \mu}{\partial N}\right)_{v(r)} \quad (2)$$

Within the framework of finite differences approximation, the following expressions based on HOMO and LUMO energy values for complexes at B3LYP/GENECP level of calculation as follows[77,78]:

$$\eta = (E_{HOMO} - E_{LUMO})/2 \quad (3)$$

$$\mu = -(E_{HOMO} + E_{LUMO})/2 \quad (4)$$

$$\omega = \mu^2/2\eta \quad (5)$$

$$\chi = (E_{HOMO} + E_{LUMO})/2 \quad (6)$$

$$S = 1/2\eta \quad (7)$$

The values of all the important reactivity descriptors of the compounds under study are given in the Table 5. These descriptors are important to explain the reactivity and stability of studied compounds.

From Table 5, it is clear that among all derivatives, **S3** has highest value of η equal to 1.32 eV with the chemically hardest compound among all, whereas **S5** has the lowest value (0.92 eV) and are chemically soft and more reactive. Other synthetized derivatives order of hardness is **S2** > **S4** > **S6** > **S2**. These findings are consistent with the HOMO-LUMO band gaps of all synthesized derivatives. The electronic chemical potential (μ) value gives an idea about the charge transfer within any compound in its ground state. From Table 5, it is clear that **S4** has the highest chemical potential value (−2.53 eV), while **S5** has the lowest chemical potential (−8.7 eV) and other with order **S3** > **S6** > **S2** > **S1**.

The electrophilicity index (ω) is a thermodynamic property that measures the changes in energy when a chemical system becomes saturated by adding electrons. It plays an excellent role in describing the chemical reactivity of a system. The results from Table 5 indicate that **S4** has the lowest electrophilicity index value (0.0 eV) and is nucleophilic in nature, whereas **S3** has the highest value i.e., of 25.41 eV and is strongly electrophilic in nature and other order is **S2** > **S6** > **S1** > **S5**.

The electronegativity (**X**), describes the ability of a molecule to attract electrons towards itself in a covalent bond**.** Thus, compound **S5** possesses higher electronegativity value (8.7 eV) than all compounds so; it is the best electron acceptor and other derivatives ordered **S1** > **S2** > **S6** > **S3** > **S4**. Global softness of a molecule represents reactivity of compounds. S**5 c**omplex showed highest softness values (0.54 eV) and showed high reactivity, While **S3** showed the least value of softness (0.38 eV) with other substituted order **S2** > **S4** = **S6** > **S1** > **S3**.

3.7.6 | Local reactivity descriptor

The concepts of local and global reactivity descriptors have been widely used to understand the chemical reactivity and site selectivity[81,82] and to analyze local molecular site selectivity of the molecules. Yang and Mortier (1986) defined the Fukui function as the first derivative of the electronic density ρ(r) of a system with respect to the number of electrons (N) at a fixed external potential ν(r)[83] as given these Equation:

$$f_k = \left(\frac{\partial \rho(r)}{\partial N}\right)_{v(r)} = \frac{1}{2}\left(\frac{\partial \mu}{\partial v(r)}\right)_{v(r)} \quad (8)$$

Parr and Yang[84] define local descriptors such as electrophilic and nucleophilic Fukui functions. Thus, calculating Fukui functions can enable us to determine the active sites of a molecule, based on the electronic density changes experienced by the molecule during a reaction.

TABLE 5 Reactivity indices of synthesized formazan compounds **(S1-S6)**

Compounds	Chemical hardness, η (eV)	Chemical potential, μ (eV)	Electrophilicity Index, ω (eV)	Electronegativity X, eV	Global softness S, eV
H_2L **(S1)**	1.26	−4.87	3.03	4.87	0.40
Cu (II) **(S2)**	1.07	−4.83	22.94	4.83	0.47
Fe (II) **(S3)**	1.32	−4.45	25.41	4.45	0.38
Cr (III) **(S4)**	1.19	−2.53	0.00	2.53	0.42
Co (III) **(S5)**	0.92	−8.70	1.85	8.70	0.54
Ni (II) **(S6)**	1.20	−4.55	3.56	4.55	0.42

Values are mean ± SD triplicate assays.

TABLE 6 Fukui and Dual descriptors of formazan compounds H_2L **(S1),** Cu (II) **(S2),** Fe (II) **(S3),** Co (III) **S5** and Ni (II) **(S6)** at B3LYP/GENECP level

	H_2L (S1)			Cu (II) (S2)			Fe (II) (S3)			Co (III) (S5)			Ni (II) (S6)		
Atoms	f_k^-	f_k^+	Δf_k	f_k^-	f_k^+	Δf_k	f_k^-	f_k^+	Δf_k	f_k^-	f_k^+	Δf	f_k^-	f_k^+	Δf_k
C1	0.008	**0.015**	**0.007**	**0.053**	0.004	**−0.049**	**0.042**	0.003	**−0.040**	**0.067**	0.003	**−0.065**	**0.043**	0.006	**−0.038**
C2	0.014	**0.085**	**0.071**	0.018	**0.075**	**0.057**	0.023	**0.074**	**0.051**	0.012	**0.059**	**0.048**	0.023	**0.078**	**0.055**
C4	0.017	**0.071**	**0.054**	0.030	**0.034**	**0.005**	0.034	0.026	−0.008	**0.034**	0.037	**0.003**	0.031	**0.033**	**0.002**
C6	0.016	**0.036**	**0.021**	**0.043**	0.024	**−0.019**	**0.042**	0.015	**−0.027**	**0.053**	0.032	**−0.021**	**0.040**	0.020	**−0.020**
O7	0.006	**0.007**	**0.001**	**0.040**	0.009	**−0.031**	**0.028**	0.007	**−0.021**	**0.050**	0.017	**−0.033**	**0.035**	0.008	**−0.027**
N11	0.000	0.001	0.000	0.003	0.006	0.003	0.002	0.007	0.005	0.002	0.003	0.001	0.002	0.006	0.004
N14	0.052	**0.205**	**0.154**	0.071	**0.170**	**0.098**	0.088	**0.150**	**0.062**	0.061	**0.151**	**0.090**	0.087	**0.160**	**0.072**
N15	0.002	**0.203**	**0.202**	0.005	**0.200**	**0.195**	0.003	**0.185**	**0.181**	0.003	**0.207**	**0.204**	0.006	**0.204**	**0.198**
C16	**0.105**	0.024	**−0.080**	**0.100**	0.012	**−0.088**	**0.116**	0.013	**−0.103**	**0.098**	0.010	**−0.088**	**0.114**	0.011	**−0.103**
N17	0.077	**0.161**	**0.084**	0.047	**0.170**	**0.122**	0.046	**0.168**	**0.122**	0.049	**0.201**	**0.152**	0.038	**0.173**	**0.135**
N18	**0.169**	0.052	**−0.117**	**0.149**	0.100	**−0.048**	**0.145**	0.098	**−0.046**	0.118	**0.128**	**0.010**	**0.151**	0.112	**−0.039**
C19	0.012	0.009	−0.003	0.012	0.019	0.007	0.010	0.016	0.006	0.015	−0.002	−0.017	0.009	**0.012**	**0.003**
C20	0.053	0.017	−0.036	0.035	0.028	−0.007	0.020	0.036	0.016	0.024	0.021	−0.003	0.037	0.027	−0.010
S29	0.005	0.005	−0.001	0.003	0.008	0.005	0.003	0.012	0.009	0.001	0.002	0.001	0.003	0.008	0.005
C34	**0.081**	0.000	**−0.081**	**0.048**	0.005	**−0.043**	**0.050**	0.000	**−0.050**	**0.054**	0.001	**−0.053**	**0.055**	0.001	**−0.054**
C35	0.061	0.006	−0.055	**0.047**	−0.013	**−0.060**	**0.051**	−0.008	**−0.059**	**0.050**	−0.001	**−0.051**	**0.045**	−0.009	**−0.053**
C37	**0.109**	0.005	**−0.104**	**0.075**	−0.001	**−0.076**	**0.082**	−0.001	**−0.082**	**0.090**	0.000	**−0.090**	**0.076**	−0.001	**−0.077**
Cu45				**0.025**	0.012	**−0.013**	**0.049**	0.042	**−0.007**	0.032	**0.038**	**0.006**	**0.025**	0.009	**−0.016**
O46				−0.001	0.000	0.001	−0.001	0.000	0.001	−0.003	0.000	0.003	−0.005	0.002	0.007
O49				0.000	0.000	0.000	0.000	0.000	0.000	−0.002	0.000	0.002	−0.005	0.000	0.005
O52				0.002	0.000	−0.003	0.002	0.000	−0.002	0.000	0.000	0.000	0.000	0.000	0.000

Values are mean ± SD triplicate assays.

Fukui functions f_k^-, f_k^+, f_k^o and Δf_k are calculated for three chemical situations, using the following equations as[85–87]:

$f_k^- = q_k(N) - q_k(N-1) \approx \rho^{HOMO}(r)$ for electrophilic attack

$f_k^+ = q_k(N+1) - q_k(N) \approx \rho^{LUMO}(r)$ for nucleophilic attack

$f_k^o = \frac{1}{2}[q_k(N+1) - q_k(N-1)] \approx \frac{1}{2}[\rho^{HOMO}(r) + \rho^{LUMO}(r)]$ for Radical attack

Where $q_k(N)$ is the atomic population on the k_{th} atom for the neutral molecule, while $q_k(N+1)$ and $q_k(N-1)$ are the atomic population on the k_{th} atom for its anionic and cationic species, respectively. As it is known, the concept of generalized philicity have been introduced by Chattaraj et al.[88] they defined a local quantity called philicity associated with a site k in a molecule with the assistance of corresponding condensed-to-atom variants of Fukui function, f_k^α as in Equation (9).

$$\omega_k^\alpha = \omega f_k^\alpha \tag{9}$$

Where $\alpha = +, -$ and 0 corresponds to local philic quantities describing nucleophilic, electrophilic and radical attacks, respectively. In the light of Equation (9), the highest ω_k^α corresponds to the most electrophilic site in a molecule. In addition, Lee et al.[89] proposed different local softness, which can be used to describe the reactivity of atoms in molecules, which can be defined as in Equation (10).

$$s_k^\alpha = s f_k^\alpha \tag{10}$$

Where $\alpha = +, -$ and 0 represents local softness quantities describing nucleophilic, electrophilic and radical attacks respectively. In addition to the information concerning electrophilic and nucleophilic capacity of a given atomic site in the molecule, Morell and Labbe et al.[90] proposed another Dual descriptor (Δf_k) which is given by:

$$\Delta f_k = f_k^+ - f_k^- \tag{11}$$

if $\Delta f_k > 0$, then the site is favored for a nucleophilic attack, whereas if $\Delta f_k < 0$, then the site may be favored for an electrophilic attack. The calculation of Fukui functions indices, local philicity, local softness and Dual

TABLE 7 Fukui and Dual descriptors of synthesized formazan compound Cr (III) (**S4**) at B3lyp/GENECP level

Atoms	f_k^-	f_k^+	Δf_k	Atoms	f_k^-	f_k^+	Δf_k
C1	**0.006**	0.001	**−0.005**	C39	0.010	0.005	−0.005
C2	0.006	0.050	0.044	Cr45	**0.199**	0.044	**−0.155**
C3	0.001	0.003	0.002	C46	0.006	0.001	−0.005
C4	0.014	0.012	−0.003	C47	0.006	0.050	0.044
C5	0.001	0.009	0.008	C48	0.001	0.003	0.002
C6	0.002	0.010	0.009	C49	0.014	0.012	−0.003
O7	**0.007**	0.002	**−0.005**	C50	0.001	0.009	0.008
N14	0.034	**0.070**	**0.037**	C51	0.002	0.010	0.009
N15	0.013	**0.096**	**0.083**	O52	0.007	0.002	−0.005
C16	**0.055**	0.009	**−0.046**	N59	0.034	**0.070**	**0.037**
N17	0.045	**0.083**	**0.038**	N60	0.013	**0.096**	**0.083**
N18	**0.069**	0.023	**−0.046**	C61	0.055	0.009	−0.046
C19	0.026	0.004	−0.022	N62	0.045	**0.083**	**0.038**
C20	0.023	0.010	−0.013	N63	**0.069**	0.023	**−0.046**
C21	0.002	0.010	0.007	C64	0.026	0.004	−0.022
C22	0.022	0.021	−0.002	C65	0.023	0.010	−0.013
C23	0.000	0.004	0.004	C66	0.002	0.010	0.007
C34	0.008	−0.013	−0.021	C67	0.022	0.021	−0.002
C35	0.014	0.005	−0.009	C68	0.000	0.004	0.004
C36	0.002	0.005	0.003	C79	0.008	−0.013	−0.022
C37	0.018	0.001	−0.017	C80	0.014	0.005	−0.009
C38	0.001	0.005	0.004	C84	0.010	0.005	−0.005

Values are mean ± SD triplicate assays.

TABLE 8 Values of the Condensed local Softnesses (Hartree*e) of formazan compounds H_2L **(S1),** Cu (II) **(S2),** Fe (II) **(S3),** Cr (III) **S4,** Co (III) **S5** and Ni (II) **(S6)** at B3LYP/GENECP level of calculation from CDFT point of view

	H2L (S1)		Cu (II) (S2)		Fe (II) (S3)		Co (III) (S5)		Ni (II) (S6)		Cr (III) (S4)				
Atoms	**s-**	**s+**	**s-**	**s+**	**s-**	**s+**	**s-**	**s+**	**s-**	**s+**	**s-**	**s+**	**Atoms**	**s-**	**s+**
C1	−0.063	−0.038	−0.018	−0.119	−0.016	−0.032	−0.044	−0.196	−0.017	−0.101	−0.039	−0.117	C46	−0.040	−0.040
C2	−0.201	−0.087	−0.200	−0.094	−0.174	−0.082	−0.130	−0.105	−0.208	−0.103	−0.039	−0.117	C49	−0.033	−0.032
C4	−0.264	−0.182	−0.196	−0.194	−0.153	−0.161	−0.182	−0.094	−0.194	−0.193	−0.111	−0.082	O52	−0.049	−0.047
C6	−0.113	−0.093	−0.084	−0.138	−0.052	−0.053	−0.103	−0.119	−0.076	−0.132	−0.147	−0.050	N56	−0.041	−0.035
O7	−0.058	−0.043	−0.108	−0.182	−0.080	−0.126	−0.145	−0.472	−0.092	−0.172	−0.050	−0.125	O57	−0.055	−0.056
N11	−0.041	−0.026	−0.072	−0.047	−0.071	−0.040	−0.049	−0.053	−0.075	−0.047	0.029	0.017	C64	−0.007	−0.082
N14	−0.429	−0.208	−0.317	−0.166	−0.255	−0.151	−0.215	0.050	−0.321	−0.199	−0.049	−0.053	C65	−0.007	−0.082
N15	−0.466	−0.026	−0.386	−0.032	−0.334	−0.230	−0.372	−0.168	−0.428	−0.032	−0.007	−0.012	C66	−0.003	−0.010
C16	−0.138	−0.266	−0.124	−0.263	−0.118	−0.173	−0.019	−0.017	−0.115	−0.297	−0.049	−0.055	C67	−0.047	−0.060
N17	−0.377	−0.101	−0.355	−0.111	−0.311	−0.214	−0.397	−0.103	−0.372	−0.087	−0.010	−0.017	C68	0.001	−0.029
N18	−0.158	−0.349	−0.206	−0.321	−0.158	−0.167	−0.238	−0.091	−0.224	−0.338	−0.081	−0.100	O77	0.001	−0.029
C19	−0.035	−0.049	−0.041	−0.001	−0.056	0.025	0.009	0.003	−0.038	−0.007	−0.042	−0.045	C82	−0.053	−0.053
C20	−0.092	−0.162	−0.092	−0.091	−0.086	−0.046	−0.074	−0.033	−0.103	−0.120	−0.043	−0.046	C83	−0.037	−0.034
S29	−0.085	−0.067	−0.093	−0.056	−0.089	−0.048	−0.053	−0.032	−0.094	−0.060	−0.081	−0.100	C84	−0.054	−0.034
C34	0.046	−0.134	0.048	−0.102	0.043	0.018	−0.019	−0.140	0.048	−0.084	−0.009	−0.023			
C35	−0.048	−0.167	−0.037	−0.153	−0.032	−0.065	−0.054	−0.084	−0.034	−0.148	−0.042	−0.055			
C37	−0.149	−0.321	−0.143	−0.294	−0.126	−0.164	−0.168	−0.239	−0.144	−0.285	−0.002	−0.004			
M45			−0.281	−0.220	−0.262	−0.774	−0.155	−0.149	−0.184	−0.114	−0.042	−0.055			
O46			−0.028	−0.051	−0.028	−0.056	0.000	−0.011	−0.029	−0.038					
O49			0.001	0.001	−0.001	−0.002	0.000	−0.007	−0.031	−0.041					
O52			−0.011	−0.017	−0.010	−0.041	−0.028	−0.029	−0.027	−0.029					

Values are mean ± SD triplicate assays.

TABLE 9 Values of relative electrophilicity/nucleophilicity (dimensionless) of formazan compounds H_2L (**S1**), Cu (II) (**S2**), Fe (II) (**S3**), Cr (III) **S4**, Co (III) **S5** and Ni (II) (**S6**) at B3LYP/GENECP level of calculation from CDFT point of view

	H2Lb (S1)		Cu (II) (S2)		Fe (II) (S3)		Co (III) (S5)		Ni (II) (S6)		Cr (III) (S4)				
Atoms	**s+/s-**	**s−/s+**	**s+/s-**	**s−/s+**	**s+/s-**	**s−/s+**	**s+/s-**	**s−/s+**	**s+/s-**	**s−/s+**	**s+/s-**	**s−/s+**		**s+/s-**	**s−/s+**
C1	0.61	**1.65**	6.77	0.15	1.95	0.51	4.43	0.23	5.89	0.17	**2.99**	0.33	C46	1.00	1.00
C2	0.43	**2.31**	0.47	2.13	0.47	2.11	0.81	1.24	0.50	2.01	**2.99**	0.33	C49	0.97	1.03
C4	0.69	1.46	0.99	1.01	1.06	0.95	0.52	1.94	1.00	1.00	0.74	1.36	O52	0.95	1.05
C6	0.82	1.22	1.64	0.61	1.03	0.97	1.16	0.86	1.73	0.58	0.34	**2.97**	N56	0.85	1.17
O7	0.74	1.35	1.69	0.59	1.58	0.63	3.26	0.31	1.87	0.53	**2.48**	0.40	O57	1.01	0.99
N11	0.62	1.60	0.65	1.55	0.56	1.78	1.07	0.94	0.63	1.60	0.58	**1.73**	C64	**11.75**	0.09
N14	0.48	2.07	0.52	1.91	0.59	1.69	−0.23	−4.30	0.62	1.61	1.07	0.94	C65	11.76	0.09
N15	0.06	**18.10**	0.08	**11.99**	0.69	**1.46**	0.45	**2.21**	0.07	**13.54**	1.88	0.53	C66	3.22	0.31
C16	1.92	0.52	**2.13**	0.47	1.47	0.68	0.94	1.07	**2.59**	0.39	1.11	0.90	C67	1.28	0.78
N17	0.27	**3.72**	0.31	3.20	0.69	1.45	0.26	3.84	0.23	4.26	1.72	0.58	C68	**−46.16**	−0.02
N18	2.21	0.45	1.56	0.64	1.06	0.95	0.38	2.63	1.51	0.66	1.25	0.80	O77	**−46.15**	−0.02
C19	1.39	0.72	0.02	**44.74**	−0.44	−2.26	0.31	3.22	0.19	5.27	1.07	0.94	C82	1.00	1.00
C20	1.76	0.57	0.99	1.01	0.54	**1.86**	0.45	2.23	1.16	0.86	1.09	0.92	C83	0.91	1.09
S29	0.79	**1.26**	0.60	1.67	0.53	**1.87**	0.60	1.66	0.64	1.55	1.25	0.80	C84	0.63	1.58
C34	−2.92	−0.34	−2.11	−0.47	0.42	**2.41**	7.59	0.13	−1.73	−0.58	**2.65**	0.38			
C35	**3.45**	0.29	**4.18**	0.24	**2.01**	0.50	1.56	0.64	**4.34**	0.23	1.30	0.77			
C37	**2.16**	0.46	**2.05**	0.49	1.31	0.77	1.42	0.70	1.98	0.51	1.94	0.52			
M45			0.78	1.28	**2.96**	0.34	0.96	1.05	0.62	1.61	1.30	0.77			
O46			1.81	0.55	**2.02**	0.49	**28.10**	0.04	1.30	0.77					
O49			0.98	1.02	1.38	0.72	**26.03**	0.04	1.32	0.76					
O52			1.60	0.63	**4.07**	0.25	1.07	0.94	1.06	0.94					

Values are mean ± SD triplicate assays.

TABLE 10 Values of the Condensed local electrophilicity/nucleophilicity index (e*eV) of formazan compounds H2L (**S1**), Cu (II) (**S2**), Fe (II) (**S3**), Cr (III) **S4**, Co (III) **S5** and Ni (II) (**S6**) at B3LYP/GENECP level of calculation from CDFT point of view

	H2L (S1)		Cu (II) (S2)		Fe (II) (S3)		Co (III) (S5)	
Atoms	**Electrophilicity**	**Nucleophilicity**	**Electrophilicity**	**Nucleophilicity**	**Electrophilicity**	**Nucleophilicity**	**Electrophilicity**	**Nucleophilicity**
C1	−0.016	−0.034	−0.048	−0.010	−0.013	−0.011	−0.237	0.000
C2	−0.037	−0.111	−0.038	−0.113	−0.032	−0.115	−0.127	0.001
C4	−0.078	−0.146	−0.078	−0.111	−0.063	−0.101	−0.114	0.001
C6	−0.040	−0.062	−0.056	−0.047	−0.021	−0.034	−0.145	0.000
O7	−0.018	−0.032	−0.073	−0.061	−0.050	−0.053	−0.573	0.001
N11	−0.011	−0.023	−0.019	−0.041	−0.016	−0.047	−0.064	0.000
N14	−0.089	−0.236	−0.067	−0.179	−0.059	−0.169	0.061	0.001
N15	−0.011	−0.256	−0.013	−0.218	−0.090	−0.221	−0.204	0.002
C16	−0.114	−0.076	−0.106	−0.070	−0.068	−0.078	−0.021	0.000
N17	−0.044	−0.208	−0.045	−0.200	−0.084	−0.206	−0.126	0.002
N18	−0.150	−0.087	−0.129	−0.116	−0.065	−0.104	−0.110	0.001
C19	−0.021	−0.019	0.000	−0.023	0.010	−0.037	0.004	0.000
C20	−0.070	−0.051	−0.037	−0.052	−0.018	−0.057	−0.040	0.000
S29	−0.029	−0.047	−0.022	−0.052	−0.019	−0.059	−0.039	0.000
C34	−0.058	0.025	−0.041	0.027	0.007	0.029	−0.170	0.000
C35	−0.072	−0.027	−0.062	−0.021	−0.026	−0.021	−0.102	0.000
C37	−0.138	−0.082	−0.118	−0.081	−0.065	−0.083	−0.290	0.001
M45			−0.089	−0.159	−0.305	−0.173	−0.180	0.001
O46			−0.020	−0.016	−0.022	−0.018	−0.014	0.000
O49			0.000	0.000	−0.001	−0.001	−0.009	0.000
O52			−0.007	−0.006	−0.016	−0.007	−0.036	0.000

TABLE 10 Values of the Condensed local electrophilicity/nucleophilicity index (e*eV) of formazan compounds H2L (**S1**), Cu (II) (**S2**), Fe (II) (**S3**), Cr (III) **S4**, Co (III) **S5** and Ni (II) (**S6**) at B3LYP/GENECP level of calculation from CDFT point of view

	Ni (II) (S6)		Cr (III) (S4)				
Atoms	**Electrophilicity**	**Nucleophilicity**	**Electrophilicity**	**Nucleophilicity**		**Electrophilicity**	**Nucleophilicity**
C1	−0.038	−0.010	−0.013	−0.047	C46	−0.004	−0.048
C2	−0.038	−0.122	−0.013	−0.047	C49	−0.003	−0.039
C4	−0.072	−0.114	−0.009	−0.134	O52	−0.005	−0.059
C6	−0.049	−0.045	−0.005	−0.177	N56	−0.004	−0.049
O7	−0.064	−0.054	−0.013	−0.060	O57	−0.006	−0.067
N11	−0.017	−0.044	0.002	0.035	C64	−0.009	−0.008
N14	−0.074	−0.189	−0.006	−0.059	C65	−0.009	−0.008
N15	−0.012	−0.252	−0.001	−0.008	C66	−0.001	−0.004
C16	−0.111	−0.068	−0.006	−0.059	C67	−0.006	−0.056
N17	−0.033	−0.219	−0.002	−0.012	C68	−0.003	0.001
N18	−0.126	−0.132	−0.011	−0.097	O77	−0.003	0.001
C19	−0.003	−0.023	−0.005	−0.051	C82	−0.006	−0.064
C20	−0.045	−0.061	−0.005	−0.051	C83	−0.004	−0.044
S29	−0.022	−0.055	−0.011	−0.097	C84	−0.004	−0.065
C34	−0.031	0.029	−0.002	−0.011			
C35	−0.055	−0.020	−0.006	−0.051			
C37	−0.107	−0.085	0.000	−0.002			
M45	−0.043	−0.108	−0.006	−0.051			
O46	−0.014	−0.017					
O49	−0.015	−0.018					
O52	−0.011	−0.016					

Values are mean ± SD triplicate assays.

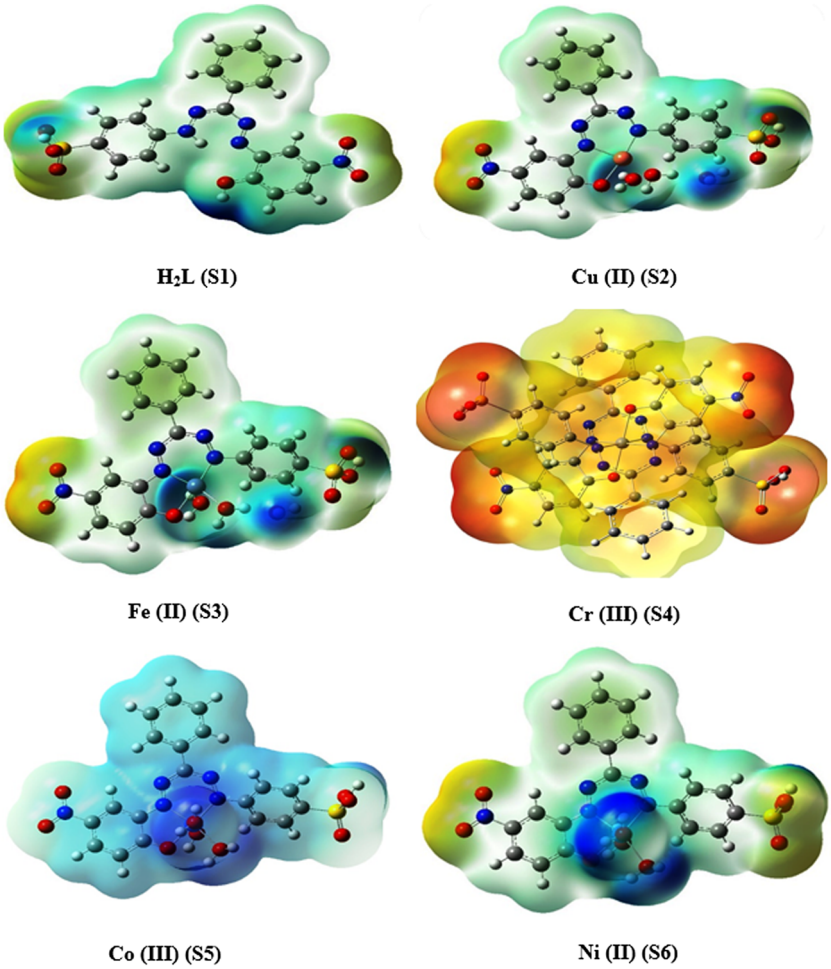

FIGURE 3 MEP surfaces of the newly synthesized formazan compounds (**S1-S6**)

TABLE 11 The MEP analysis of synthesized formazan compounds (**S1-S6**)

Compounds	+ve potential	-ve potential
H_2L **(S1)**	0.095	−0.095
Cu (II) **(S2)**	0.084	−0.084
Fe (II) **(S3)**	0.085	−0.085
Cr (III) **(S4)**	0.111	−0.111
Co (III) **(S5)**	0.177	−0.177
Ni (II) **(S6)**	0.088	−0.088

Values are mean ± SD triplicate assays

descriptor of the studied molecules **S1-S6** at the level B3LYP/GENECP is given in Table 6–10.

From the values of Fukui functions f_k^- and f_k^+, it can be stated that the most electrophilic active site in ligand molecule is located on C16, N18, C34, C35 and C37. Likewise, the active sites susceptible for nucleophilic attacks are C1, C2, C4, C6, O7, N14, N15 and N17. The same conclusion can be reached considering the Dual descriptor Δf_k regarding electrophilic and nucleophilic attack. These results are completely changed when the chelation formed with central metal ions. In case of synthesized formazan compounds **S2, S3** and **S6**, the most electrophilic active sites are located on C1, C6, O7, C16, C34, C35, C37 and M45. While nucleophilic attacks are on C2,

C4, N14, N15 and N17, the reason of these characteristic differences is the redistribution of electron density inside molecules due to chelation form, high electronegativity of N and O atoms in coordination centers also the effect of -NO_2, -SO_3H substituted groups.

In case of **S5** compounds, the Co45 and N18 pattern changed from electrophilic to nucleophilic attack due to back donation of Co atom to the center atoms. These results mixed with the same last in **S1, S3** and **S6**. In case of **S4**, the most electrophilic active sites are located on C1, O7, C16, N18, Cr45 and N63 while nucleophilic attacks are N14, N15, N17, N59, N60 and N62, which is almost results in all complexes except **S5** chelation. These results are in agreement with the last population analysis part with computed HOMO and LUMO.

To complete the picture, the condensed local softness, local electrophilicity/nucleophilicity index, and relative electrophilicity/nucleophilicity have been also calculated for each atoms in the studied molecules from CDFT point of view by using implemented code in Multiwfn v3.7 software program.[91] A close inspection would reveal that all the molecules had the donating and the back-donation process at their chelated center (C1, C6, O7, M, N14, N15, C16, N17 and N18) in agreement with the frontier orbital results obtained. According to these results, one can conclude that proposed molecules will have many active centers to interact with pocket protein surface, through donating electrons to the metal ions 3d orbitals and back donation process. Finally, the above local descriptors reveal that the theoretical variation of the efficiencies of the investigative molecules agrees with the available experimental data in the same work.

3.7.7 | Molecular electrostatic potential (MEP)

MEP analysis with the help of quantum mechanical methods has been used extensively to explain the reactive sites within compounds **(S1-S6)**. MEP is found to be a useful descriptor to predict reactive sites for electrophilic and nucleophilic attack reactions as well as hydrogen-bonding interactions.[92,93] With MEP analysis, the reactive sites can be located by different color codes, such as the red color in a MEP graphic indicates an electron-rich site, blue color indicates an electron-deficient site, while the green color is indicative of a neutral region. The MEP analysis of compounds *viz.* **S1-S6** was carried out. Figure 3 displayed the MEP surfaces of the newly synthesized derivatives S1-S6, while the corresponding +ve and –ve potential values from the MEP analysis of these compounds are given in Table 11, which indicate the same results from NBO population and local Fukui descriptors analysis.

4 | CONCLUSION

The superior antibacterial and antimycotic activities were exhibited by formazan compound **(S4)** by presenting maximum ZOIs and MICs values. While substantial and enhanced antioxidant in terms of percentage inhibition of DPPH and cytotoxic effect on human breast carcinoma cells was demonstrated by formazan compound **(S1)** which was further validated by the results of molecular docking studies of **(S1)** with the human estrogen receptor protein. To explore the structural properties, Density functional theory (DFT) investigations on all synthesized complexes **(S1-S6)** were performed. Frontier molecular orbitals (FMO) analysis reveals that the spread of isodensity was mainly concentrated on the phenyl ring of ligand and groups directly attached. The computational results also show that C16, N18, C34, C35 and C37 are the most preferred sites for electrophilic attack. Likewise, the active sites susceptible for nucleophilic attacks are C1, C2, C4, C6, O7, N14, N15 and N17. The HOMO/LUMO band gap studies and MEP analysis revealed the reactivity and the binding of complexes as a drug to the protein actives sites. The formazans compounds could be potential drug candidate that constrains the growth of microbial strains, possess ability to cause cytotoxic effect on carcinoma cells and act as effective scavenger for free radical species.

ACKNOWLEDGMENTS

This work was supported by the Department of Chemistry, School of Science, University of Management and Technology, Lahore, Pakistan and Shafi Reso Chemical Lahore, Pakistan.

CONFLICT OF INTEREST

No conflict of interest associated with this work.

CONTRIBUTIONS OF AUTHORS

The authors declare that this work was done by the authors named in this article. The authors Shakeel Ahmad Khan has done the experimental work and Sammia Shahid supervised the whole research work. Mahmoud A. Noamaan, Komal Rizwan, Tahir Rasheed and Hira Amjad assisted in the docking and DFT with computational exploration of chemical reactivity studies of new synthesized formazn compounds respectively.

DECLARATIONS

ORCID

Shakeel Ahmad Khan https://orcid.org/0000-0002-7594-1222
Tahir Rasheed https://orcid.org/0000-0001-9265-6303

REFERENCES

[1] K. S. Sunil, C. Usha, *Asian J. Pharm. Clin. Res.* **2018**, *11*, 398.
[2] A. Subramanian, N. Kannan, P. Mani, *Int. J. Curr. Pharm. Res.* **2017**, *9*, 85.
[3] N. Mulcahy, Cancer to Become Leading Cause of Death Worldwide by 2010. Medscape Medical News, **2008**.
[4] L. Hong, G. P. Schroth, H. R. Matthews, P. Yau, E. M. Bradbury, *J. Biol. Chem.* **1993**, *268*, 305. PMID: 8416938
[5] H. Patel, P. Sinha, *Curr. Sci.* **2001**, *81*, 641.
[6] R. Marti-Centelles, R. Cejudo-Marin, E. Falomir, J. Murga, M. Carda, J. A. Marco, *Bioorg. Med. Chem.* **2013**, *21*, 3010.
[7] M. Mahdavi, K. Pedrood, M. Safavi, M. Saeedi, M. Pordeli, S. K. Ardestani, S. Emami, M. Adib, A. Foroumadi, A. Shafiee, *Eur. J. Med. Chem.* **2015**, *95*, 492.
[8] A. S. Shawali, N. A. Samy, *J Adv Res.* **2015**, *6*, 241.
[9] S. A. Khan, S. Shahid, S. Kanwal, G. Hussain, *Dyes Pigm.* **2018**, *148*, 31.
[10] S. A. Khan, S. Shahid, S. Kanwal, K. Rizwan, T. Mahmood, K. Ayub, *J. Mol. Struct.* **2018**, *1175*, 73.
[11] D. E. Berry, R. G. Hicks, J. E. Gilroy, *J. Chem. Educ.* **2009**, *86*, 76.
[12] S. B. Chavan, S. B. Zangade, Y. Archana, Y. B. VIbhute, *J Chem Pharm Res.* **2012**, *3*, 262.
[13] M. Kidwai, N. Negi, S. D. Gupta, *Chem. Pharm. Bull.* **1994**, *42*, 2363.
[14] J. D. Bhosale, A. R. Shirolkar, U. D. Pete, C. M. Zade, D. P. Mahajan, C. D. Hadole, S. D. Pawar, U. D. Patil, R. Dabur, R. S. Bendre, *J Pharm Res.* **2013**, *7*, 582.
[15] D. D. Mukerjee, S. K. Shukla, B. L. Chowdhary, *Arch Pharm (Weinheim).* **1981**, *314*, 991.
[16] R. Khanna, G. Palit, V. K. Srivastava, K. Shanker, *Indian J. Chem.* **1990**, *29B*, 556.
[17] J. P. Raval, P. Patel, S. Pradip, P. S. Patel, *Int J Pharm Tech Res.* **2009**, *1*, 1548.
[18] A. Srivastava, A. V. Kumar, *Indian J. Pharm. Sci.* **2001**, *65*, 358.
[19] S. D. Bhardwaj, *Asian J. Chem.* **1998**, *10*, 39.
[20] S. D. Bhardwaj, V. S. Jolly, *Asian J. Chem.* **1997**, *9*, 48.
[21] H. A. Mahdi, K. S. Abbas, H. M. Dagher, *Chem Mat Res.* **2015**, *7*, 72.
[22] A. S. Yaglıoglu, H. Senoz, *Hacettepe J Biol Chem.* **2013**, *41*, 371.
[23] R. Kaisi, K. Pande, T. N. Bhalla, J. P. Barthwal, G. P. Gupta, S. S. Parmar, *J. Pharm. Sci.* **1990**, *79*, 317.
[24] D. J. Knowles, *Trends Microbiol.* **1997**, *5*, 379.
[25] C. R. Harris, A. Thorarensen, *Curr. Med. Chem.* **2004**, *11*, 2213.
[26] I. Chopra, J. Hodgson, B. Metcalf, G. Poste, *JAMA* **1996**, *275*, 401.
[27] N. Singh, S. K. Bhati, A. Kumar, *Eu J Med Chem.* **2008**, *43*, 2597.
[28] P. Thangavelu, S. Chellappa, S. Thangavel, *Int J Pharm Pharm Sci.* **2018**, *10*, 56.
[29] K. Hunger, *Industrial Dyes: Chemistry, Properties, Applications*, Wiley-VCH, Germany **2003** 1.
[30] F. E. H. David, L. Blangey, *Fundamental processes of dye chemistry*, Interscience publisher's ltd., London **1949** 1.
[31] Y. Gu, F. Jérôme, *Chem. Soc. Rev.* **2013**, *42*, 9550.
[32] J. Yang, H. Q. Li, M. H. Li, J. J. Peng, Y. L. Gu, *Adv Synth Catal.* **2012**, *354*, 688.
[33] M. Zhang, Z. R. Shang, X. T. Li, J. N. Zhang, Y. Wang, K. Li, Y. Y. Li, Z. H. Zhang, *Synth. Commun.* **2017**, *47*, 178.
[34] R. Y. Guo, Z. M. An, L. P. Mo, R. Z. Wang, H. X. Liu, S. X. Wang, Z. H. Zhang, *ACS Comb. Sci.* **2013**, *15*, 557.
[35] R. Y. Guo, Z. M. An, L. P. Mo, S. T. Yang, H. X. Liu, S. X. Wang, Z. H. Zhang, *Tetrahedron* **2013**, *69*, 9931.
[36] X. T. Li, A. D. Zhao, L. P. Mo, Z. H. Zhang, *RSC Adv.* **2014**, *4*, 51580.
[37] H. S. Chen, R. Y. Guo, *Monatsh. Chem.* **2015**, *146*, 1355.
[38] X. T. Li, Y. H. Liu, X. Liu, Z. H. Zhang, *RSC Adv.* **2015**, *5*, 25625.
[39] P. Geerlings, F. De Prof, W. Langenaeker, *Chem. Rev.* **2003**, *103*, 1793.
[40] F. Ijaz, S. Shahid, S. A. Khan, W. Ahmad, S. Zaman, *Trop J Pharm Res.* **2017**, *16*, 743.
[41] S. A. Khan, F. Noreen, S. Kanwal, A. Iqbal, G. Hussain, *Mater. Sci. Eng. C* **2018**, *82*, 46.
[42] S. A. Khan, N. Rasool, M. Riaz, R. Nadeem, U. Rashid, K. Rizwan, M. Zubair, I. H. Bukhari, T. Gulzar, *Asian J. Chem.* **2013**, *25*, 7457.
[43] S. A. Khan, S. Shahid, Z. A. Khan, A. Iqbal, *Int. J. Sci. And Res. Pub.* **2016**, *6*, 529.
[44] S. A. Khan, F. Noreen, S. Kanwal, G. Hussain, *Dig. J. Nanomater. Biostruct.* **2017**, *12*, 877.
[45] A. Khalid, S. Shahid, S. A. Khan, S. Kanwal, A. Yaqoob, Z. G. Rasool, K. Rizwan, *Trop J Pharm Res.* **2018**, *17*, 1531.
[46] S. A. Khan, S. Shahid, W. Ahmad, S. Ullah, *Int J Pharm Sci and Res.* **2017**, *2*, 22.
[47] S. A. Khan, S. Shahid, M. R. Sajid, F. Noreen, S. Kanwal, *Int. J. Adv. Res.* **2017**, *5*, 925.
[48] S. A. Khan, S. Kanwal, A. Iqbal, W. Ahmad, *Int. J. Adv. Res.* **2017**, *5*, 1350.
[49] S. A. Khan, M. Jameel, S. Kanwal, S. Shahid, *Int J Pharm Sci and Res.* **2017**, *2*, 29.
[50] S. A. Khan, S. Shahid, M. Jameel, A. Ahmad, *Int J Pharma Chem.* **2016**, *6*, 107.
[51] S. A. Khan, W. Ahmad, K. S. Munawar, S. Kanwal, *Indian J. Pharm. Sci.* **2018**, *80*, 480.
[52] A. Iqbal, Z. A. Khan, S. A. Shahzad, M. Usman, S. A. Khan, A. H. Fauq, A. Bari, M. A. Sajid, *Turk. J. Chem.* **2018**, *42*, 1518.
[53] S. A. Khan, S. Shahid, S. Jabin, S. Zaman, M. Sarwar, *Dig. J. Nanomater. Biostruct.* **2018**, *13*, 285.
[54] S. Shahid, S. A. Khan, W. Ahmad, U. Fatima, S. Knawal, *Indian J. Pharm. Sci.* **2018**, *80*, 173.
[55] M. A. Qamar, S. Shahid, S. A. Khan, S. Zaman, M. Sarwar, *Dig. J. Nanomater. Biostruct.* **2017**, *12*, 1127.
[56] S. A. Khan, S. Shahid, W. Bashir, S. Kanwal, A. Iqbal, *Trop J Pharm Res.* **2017**, *16*, 2331.
[57] W. Ahmad, S. A. Khan, K. S. Munawar, A. Khalid, S. Kawanl, *Trop J Pharm Res.* **2017**, *16*, 1137.
[58] K. D. Dykstra, L. Guo, E. T. Birzin, W. Chan, Y. T. Yang, E. C. Hayes, C. A. DaSilva, L. Y. Pai, R. T. Mosley, B. Kraker,

P. M. Fitzgerald, F. DiNinno, S. P. Rohrer, J. M. Schaeffer, *Bioorg. Med. Chem. Lett.* **2007**, *17*, 2322.
[59] Dassault Systèmes BIOVIA, *Biovia Discovery Studio Visualizer, v16.1.0*, San Diego, Dassault Systèmes **2016**.
[60] O. Tacar, P. Sriamornsak, C. R. Dass, *J. Pharm. Pharmacol.* **2013**, *65*, 157.
[61] G. M. Morris, R. Huey, W. Lindstrom, M. F. Sanner, R. K. Belew, D. S. Goodsell, A. J. Olson, *J. Comput. Chem.* **2009**, *30*, 2785.
[62] O. Trott, A. J. Olson, *J. Comput. Chem.* **2010**, *31*, 455.
[63] T. Sander, J. Freyss, M. von Korff, C. Rufener, *J. Chem. Inf. Model.* **2015**, *55*, 460.
[64] A. D. Becke, *Phys. Rev. a* **1988**, *38*, 3098.
[65] A. D. Becke, *J. Chem. Phys.* **1993**, *98*, 5648.
[66] B. G. Johnson, M. J. Frisch, *Chem. Phys. Lett.* **1993**, *216*, 133.
[67] C. Lee, W. Yang, R. G. Parr, *Phys. Rev. B* **1988**, *37*, 785.
[68] A. Schafer, C. Huber, R. Ahlrichs, *J. Chem. Phys.* **1994**, *100*, 5829.
[69] A. D. McLean, G. S. Chandler, *J. Chem. Phys.* **1980**, *72*, 5639.
[70] R. Ditchfield, W. J. Hehre, J. A. Pople, *J. Chem. Phys.* **1971**, *54*, 724.
[71] S. E. Ulic, C. O. D. Vedova, A. Hermann, H.-G. Mack, H. Oberhammer, *J. Phys. Chem. A* **2008**, *112*, 6211.
[72] A. E. Reed, F. Weinhold, *J. Chem. Phys.* **1983**, *78*, 4066.
[73] http://www.chemcraftprog.com.
[74] R. Dennington, T. Keith, J. Millam, *GaussView, Version 5*, Semichem Inc., Shawnee Mission, KS **2009**.
[75] L. Tian, C. Feiwu, *J. Comput. Chem.* **2012**, *33*, 580.
[76] S. S. Zumdahl, *Chemistry for Chemical and Biological Sciences*, University Science Books, Sausalito, CA **2000**.
[77] R. G. Pearson, *Proc. Natl. Acad. Sci.* **1986**, *83*, 8440.
[78] A. K. Chandra, T. Uchimara, *J. Phys. Chem. A* **2001**, *105*, 3578.
[79] S. B. Liu, *Acta Phys.-Chim. Sin.* **2009**, *25*, 590.
[80] J. Frau, D. Glossman-Mitnik, *Front. Chem.* **2017**, *5*, 16.
[81] P. Geerlings, F. De Proft, W. Langenaeker, *Chem. Rev.* **2003**, *103*, 1793.
[82] P. K. Chattaraj, D. R. Roy, *Chem. Rev.* **2007**, *107*, PR46.
[83] W. Yang, W. J. Mortier, *J. Am. Chem. Soc.* **1986**, *108*, 5708.
[84] R. G. Parr, W. Yang, *J. Am. Chem. Soc.* **1984**, *106*, 4049.
[85] R. G. Parr, R. G. Pearson, *J. Am. Chem. Soc.* **1983**, *105*, 7512.
[86] P. K. Chattaraj, S. Giri, *J. Phys. Chem. A* **2007**, *111*, 11116.
[87] R. R. Contreras, P. Fuentealba, M. Galvan, P. Perez, *Chem. Phys. Lett.* **1999**, *304*, 405.
[88] R. Parthasarathi, J. Padmanabhan, M. Elango, V. Subramanian, P. K. Chattaraj, *Chem. Phys. Lett.* **2004**, *394*, 225.
[89] C. T. Lee, W. T. Yang, R. G. Parr, *J. Mol. Struct.: THEOCHEM* **1988**, *40*, 305.
[90] C. Morell, A. Grand, A. Toro-Labbe, *J. Phys. Chem. A* **2005**, *109*, 205.
[91] J. Padmanabhan, R. Parthasarathi, V. Subramanian, P. K. Chattaraj, *J. Phys. Chem. A* **2006**, *110*, 2739.
[92] F. J. Luque, J. M. Lopez, M. Orozco, *Theor. Chem. Acc.* **2000**, *103*, 343.
[93] F. Weigend, R. Ahlrichs, *Phys. Chem. Chem. Phys.* **2005**, *7*, 3297.

SUPPORTING INFORMATION

Additional supporting information may be found online in the Supporting Information section at the end of this article.

How to cite this article: Khan SA, Rizwan K, Shahid S, Noamaan MA, Rasheed T, Amjad H. Synthesis, DFT, computational exploration of chemical reactivity, molecular docking studies of novel formazan metal complexes and their biological applications. *Appl Organometal Chem*. 2020;e5444. https://doi.org/10.1002/aoc.5444